Macrophage Scavenger Receptor 1 mediates lipid-induced inflammation in non-alcoholic fatty liver disease

Olivier Govaere[1*]†, Sine Kragh Petersen[2]‡, Nuria Martinez-Lopez[3,4]‡, Jasper Wouters[5,6], Matthias Van Haele[7], Rosellina M. Mancina[8], Oveis Jamialahmadi[8], Orsolya Bilkei-Gorzo[2], Pierre Bel Lassen[9], Rebecca Darlay[10], Julien Peltier[3], Jeremy M. Palmer[1], Ramy Younes[1,11], Dina Tiniakos[1,12], Guruprasad P. Aithal[13], Michael Allison[14], Michele Vacca[15], Melker Göransson[16], Michael J Drinnan[1], Hannele Yki-Järvinen[17], Jean-Francois Dufour[18,19], Mattias Ekstedt[20], Sven Francque[21], Salvatore Petta[22], Elisabetta Bugianesi[11], Jörn M Schattenberg[23], Christopher P. Day[1], Heather J. Cordell[10], Baki Topal[24], Karine Clément[9], Stefano Romeo[8], Vlad Ratziu[25], Tania Roskams[7], Ann K. Daly[1], Quentin M. Anstee[1,26*]†, Matthias Trost[3*]†, Anetta Härtlova[2,3*]†

Affiliations:

[1]Translational and Clinical Research Institute, Faculty of Medical Sciences, Newcastle University, Newcastle upon Tyne, United Kingdom.

[2]Wallenberg Centre for Molecular and Translational Medicine, Department of Microbiology and Immunology at Institute of Biomedicine, University of Gothenburg, Gothenburg, Sweden.

[3]Biosciences Institute, Faculty of Medical Sciences, Newcastle University, Newcastle upon Tyne, United Kingdom.

[4]Radiation Oncology, Albert Einstein College of Medicine, New York, USA.

[5]Center for Brain & Disease Research, VIB-KU Leuven, Leuven, Belgium

[6]Department of Human Genetics, KU Leuven, Leuven, Belgium

[7]Department of Imaging and Pathology, Translational Cell and Tissue Research, KU Leuven and University Hospitals Leuven, Leuven, Belgium

[8]The Wallenberg Laboratory for Cardiovascular and Metabolic Research, Department of Molecular and Clinical Medicine, University of Gothenburg, Gothenburg, Sweden.

[9] Nutrition and obesity: systemic approaches, Inserm, Sorbonne University, Paris, France.

[10]Population Health Sciences Institute, Faculty of Medical Sciences, Newcastle University, Newcastle upon Tyne, United Kingdom.

30 [11]Department of Medical Sciences, Division of Gastro-Hepatology, A.O. Città della Salute e
31 della Scienza di Torino, University of Turin, Turin, Italy.
32 [12] Department of Pathology, Aretaieio Hospital, National & Kapodistrian University of Athens,
33 Athens, Greece.
34 [13]NIHR Nottingham Biomedical Research Centre, Nottingham University Hospitals NHS Trust
35 and University of Nottingham, Nottingham, United Kingdom.
36 [14]Liver Unit, Department of Medicine, Cambridge Biomedical Research Centre, Cambridge
37 University NHS Foundation Trust, United Kingdom.
38 [15]University of Cambridge Metabolic Research Laboratories, Wellcome-MRC Institute of
39 Metabolic Science, Addenbrooke's Hospital, Cambridge, United Kingdom.
40 [16]Bioscience COPD/IPF, Research and Early Development, Respiratory and Immunology (R&I),
41 BioPharmaceuticals R&D, AstraZeneca, Gothenburg, Sweden.
42 [17]Department of Medicine, University of Helsinki, Helsinki, Finland.
43 [18]University Clinic for Visceral Surgery and Medicine, University of Bern, Bern, Switzerland.
44 [19]Hepatology, Department of Biomedical Research, University of Bern, Bern, Switzerland
45 [20]Division of Gastroenterology and Hepatology, Department of Medicine and Health Sciences,
46 Linköping University, Linkoping, Sweden.
47 [21]Department of Gastroenterology and Hepatology, Antwerp University Hospital & University of
48 Antwerp, Antwerp, Belgium.
49 [22]Sezione di Gastroenterologia, Dipartimento Biomedico di Medicina Interna e Specialistica,
50 Università di Palermo, Palermo, Italy.
51 [23]I. Department of Medicine, University Hospital Mainz, Mainz, Germany.
52 [24]Department of Abdominal Surgery, KU Leuven and University Hospitals Leuven, Leuven,
53 Belgium
54 [25]Assistance Publique-Hôpitaux de Paris, hôpital Beaujon, University Paris-Diderot, Paris,
55 France.
56 [26] Newcastle NIHR Biomedical Research Centre, Newcastle upon Tyne Hospitals NHS Trust,
57 Newcastle upon Tyne, United Kingdom.
58 †Senior authors ‡ contributed equally *Corresponding authors
59

Correspondence:
Dr. Olivier Govaere, PhD
Translational and Clinical Research Institute,
The Medical School, Newcastle University,
4th Floor, William Leech Building,
Framlington Place, Newcastle-upon-Tyne, NE2 4HH, United Kingdom
Email: olivier.govaere@newcastle.ac.uk

Dr Anetta S. Härtlova, PhD
Assistant Professor
Wallenberg Centre for Molecular and Translational Medicine
University of Gothenburg, Institute of Biomedicine
Department of Microbiology and Immunology
Medicinaregatan 7 A, 40530 Göteborg, Sweden
Email: anetta.hartlova@gu.se

Prof Matthias Trost, PhD
Biosciences Institute,
The Medical School, Newcastle University,
4th Floor, William Leech Building,
Framlington Place, Newcastle-upon-Tyne, NE2 4HH, United Kingdom
Email:matthias.trost@newcastle.ac.uk

Prof Quentin M. Anstee, PhD, FRCP
Translational and Clinical Research Institute,
The Medical School, Newcastle University,
4th Floor, William Leech Building,
Framlington Place, Newcastle-upon-Tyne, NE2 4HH, United Kingdom
Email: quentin.anstee@newcastle.ac.uk

One Sentence Summary:

The immunometabolic role of MSR1 in human NAFLD.

Abstract:

Obesity-associated inflammation is a key player in the pathogenesis of non-alcoholic fatty liver disease (NAFLD). However, the exact mechanisms remain incompletely understood. Here we demonstrate that macrophage scavenger receptor 1 (MSR1, CD204) expression is associated with the occurrence of hepatic lipid-laden foamy macrophages and correlates with the degree of steatosis and steatohepatitis in a cohort of 170 NAFLD patients. Mice lacking Msr1 are protected against high fat-cholesterol diet (HFD)-induced metabolic disorder, showing fewer hepatic lipid-laden foamy macrophages, less hepatic inflammation, improved dyslipidemia and glucose tolerance, while showing a change in hepatic lipid metabolism. We show that MSR1 induces a pro-inflammatory response via the JNK signaling pathway upon triggering by saturated fatty acids. *In vitro* blockade of the receptor prevented the accumulation of lipids in primary macrophages which inhibited the switch towards a pro-inflammatory phenotype and the release of cytokines such as TNFα. Targeting MSR1 using monoclonal antibody therapy in an obesity-associated NAFLD mouse model and *ex vivo* human liver slices resulted in the prevention of foamy macrophage formation and liver inflammation. Moreover, we identified that rs41505344, a polymorphism in the upstream transcriptional region of *MSR1*, was associated with altered serum triglycerides and aspartate transaminase levels in a cohort of over 400,000 patients. Taken together, our data suggest a critical role for MSR1 in lipid homeostasis and a potential therapeutic target for the treatment of NAFLD.

113 **Introduction**

114 With the increasing prevalence of obesity, non-alcoholic fatty liver disease (NAFLD) has
115 become the most common chronic liver disease globally (*1*). NAFLD is characterized by
116 excessive hepatic triglyceride accumulation and represents a series of diseased states ranging
117 from isolated steatosis (non-alcoholic fatty liver, NAFL) to non-alcoholic steatohepatitis
118 (NASH), identified by the presence of necro-inflammation and hepatocyte ballooning, with
119 varying degrees of fibrosis. NAFLD is strongly linked with metabolic syndrome, i.e.
120 dyslipidemia, hypertension, obesity and type 2 diabetes mellitus (T2DM), and currently affects
121 20 to 30% of the global population (*2*). Importantly, not all patients progress from NAFL to
122 NASH and although gene signatures of more advanced fibrosing-steatohepatitis have been
123 identified, the exact pathogenic pathways involved in the initiating phases of the disease,
124 especially the transition from NAFL to NASH, are not fully understood (*3*).
125
126 Growing evidence supports the view that Kupffer cells, the endogenous hepatic macrophages,
127 are initiators of inflammation and hence contribute to NAFLD development, whilst recruited
128 monocyte-derived macrophages play a crucial role in the disease progression (*4, 5*). Hepatic
129 macrophages are responsive to a variety of stimuli including bacterial endotoxins (such as
130 lipopolysaccharide) but also free fatty acids (FFAs) or cholesterol (*6*). Excess of FFAs and
131 cholesterol can cause the formation of hepatic foamy macrophages, resembling those seen in
132 atherosclerotic lesions, and leads to Kupffer cell aggregates and lipogranulomas during
133 steatohepatitis (*7, 8*). Specifically the intake of saturated fat has been shown to induce insulin
134 resistance, enhance intrahepatic triglyceride accumulation and steatohepatitis (*9*). Liver biopsies
135 from patients with metabolic NAFLD have been described to be markedly enriched in saturated
136 and monounsaturated triacylglycerols and FFAs (*10*). In advanced NASH, specific individual
137 saturated FAs (SFAs), such as myristic acid (C14:0) or palmitic acid (PA, C16:0), proved to be
138 increased when compared to earlier stages of the disease (*11*). However, the molecular
139 mechanisms underlying hepatic macrophage activation and/or the formation of lipid-laden foamy
140 macrophages in NAFLD remain poorly understood.
141
142 PA, rather than non-SFAs, has been shown to be a strong inducer of inflammation in
143 immortalized cell lines through activation of the downstream JNK signaling pathway (*12, 13*).

144 Recent data show that pro-inflammatory activation of murine bone marrow-derived macrophages
145 by PA is independent of Toll-like receptor 4, yet the receptor that is responsible is still not
146 known (*14*). Recently, we have shown that *in vitro* activation of the phagocytic receptor,
147 macrophage scavenger receptor 1 (MSR1, also known as SR-A or CD204), results in pro-
148 inflammatory macrophage polarization through JNK activation (*15*). MSR1 is a key macrophage
149 receptor for the clearance of circulating lipoproteins and has been implicated in atherogenesis
150 (*16, 17*). We therefore hypothesized that MSR1 might be involved in inflammatory responses in
151 the context of lipid overload during obesity-induced NAFLD.
152
153 Here we show that *MSR1* gene expression is associated with NAFLD disease activity in a large
154 cohort of patients with histologically proven NAFLD and that MSR1 deficiency in a mouse
155 model of obesity-associated NAFLD prevents foamy macrophage formation, and the induction
156 of liver inflammation and fibrosis. Moreover, we found that systemic administration of MSR1
157 monoclonal antibody could modify NAFLD pathology in a mouse model and human *ex vivo*
158 liver slices of obesity-associated NAFLD.
159

160 **Results**

161 *MSR1 expression correlates with steatohepatitis activity in human NAFLD*
162 As MSR1 is a receptor for lipids in macrophages, we investigated the impact of MSR1 on
163 NAFLD. We first analyzed *MSR1* gene expression in a cohort of 170 histologically characterized
164 human adult liver biopsies using nanoString transcriptomics. The cohort was stratified according
165 to histopathological disease grade and stage, i.e. NAFL and NASH with fibrosis ranging from F0
166 to F4 (**Table S1**). The analysis revealed a significant increase of *MSR1* gene expression in
167 NASH compared to NAFL ($p<0.01$), indicating a positive correlation with the active
168 inflammatory form of the disease (**Fig. 1a)**. This observation was supported by a significant
169 correlation between *MSR1* mRNA expression and steatosis grade (Spearman $r=0.29$, $p=0.0001$),
170 hepatocyte ballooning ($r=0.22$, $p<0.01$) and lobular inflammation ($r=0.24$, $p<0.01$), while there
171 was no correlation with stages of hepatic fibrosis indicating that *MSR1* mRNA are strongly
172 linked to steatohepatitis activity rather than wound healing *per se* (**Fig. 1b**) . In addition, *MSR1*
173 mRNA correlated with the NASH Clinical Research Network NAFLD Activity Score (NAS),

174 defined as the sum of steatosis, ballooning and lobular inflammation (r=0.35, p<0.0001, **Fig.**
175 **S1a**) (*18*). Patients with NAS≥4 showed a significant increase in MSR1 expression (fold change
176 =1.34, p<0.0001, **Fig. S1a**). Furthermore, *MSR1* positively correlated with serum levels of
177 alanine transaminase (ALT, r=0.31, p=0.0001) and aspartate transaminase (AST, r=0.32,
178 p<0.0001) (**Fig. S1b**). Histopathological analysis of human adult NAFLD liver biopsies showed
179 that MSR1 was predominantly expressed in resident liver macrophages, the Kupffer cells, rather
180 than infiltrating monocyte-derived macrophages located in the portal tract, as visualized by the
181 MSR1 and CD68 immunostaining (**Fig. 1c and Fig. S2a-b**) . While the number of infiltrating
182 portal CD68-immunopositive cells increased with disease progression (p<0.05), no significant
183 differences were found for infiltrating MSR1-positive cells (**Fig.1c**). These results were
184 confirmed using publicly available single cell RNA sequencing data from healthy and end-stage
185 cirrhotic liver, showing that *MSR1* expression was mainly restricted to the Kupffer cell
186 population, whereas *CD68* or the expression of other scavenger receptors, such as *CD36*, was
187 also found in monocyte populations (**Fig. S2c**) (*19*). Notably, MSR1 immunopositivity was seen
188 in lipid-laden foamy macrophages and lipogranulomas throughout the spectrum of NAFLD,
189 indicating a role for MSR1 in lipid accumulation in endogenous macrophages and concordantly
190 inflammation (**Fig. 1c and Fig. S2d**).

191 As macrophages have been reported to regulate metabolic homeostasis in adipose tissue (*20*), we
192 evaluated MSR1 expression in subcutaneous and matched omental adipose tissue from obese
193 patients (BMI >30 kg/m^2). MSR1-immunopositive macrophages were observed in crown-like
194 structures in both types of adipose tissue, though no association was found between MSR1-
195 immunopositive cells present in the adipose tissue and the diagnosis of NASH (**Fig. 1d and Fig.**
196 **S2e**). Taken together, these human data demonstrate a positive correlation of *MSR1* transcript
197 and protein levels with obesity-associated NAFLD and occurrence of hepatic-resident lipid-laden
198 macrophages in the presence of excess lipid accumulation.
199

200 *Msr1 deficiency protects against diet-induced metabolic dysregulation and liver damage in mice*
201 To further investigate how MSR1 functionally contributes to the development of obesity-related
202 NAFLD, we subjected *Msr1*$^{-/-}$ mice (n=5) and their corresponding *Msr1*$^{+/+}$ (n=5, wild-type, WT)
203 male and age-matched counterparts to a high-fat and high-cholesterol diet (HFD) for 16 weeks.
204 Upon HFD feeding, *Msr1*-deficient mice displayed an increased total body weight and an

205 increase in liver and epididymal white adipose tissue (eWAT) weight compared to WT ($p<0.05$,
206 **Fig. 2a-b**). Consistent with enhanced adipose mass, HFD-fed *Msr1*$^{-/-}$ mice displayed enhanced
207 fatty acid accumulation within the cells ($p<0.0001$, **Fig. 2c**) along with larger adipocytes
208 compared to WT mice ($p<0.0001$, **Fig. 2d-e**), indicating an increased adiposity and fat storage in
209 the absence of *Msr1*. Although no murine models accurately recapitulate all histological features
210 of human steatohepatitis (*21*), histological and transcriptomic features of liver fibrosis were
211 clearly attenuated by *Msr1* deficiency upon HFD feeding (**Fig. 2d-f**). Sixteen weeks of regular
212 diet did not result in any histological differences between the livers of WT and *Msr1*$^{-/-}$ mice (**Fig.**
213 **S3a**), while WT mice on HFD displayed a significant higher hepatic fibrosis stage ($p<0.05$, **Fig.**
214 **S3a-b**) and increased collagen deposition ($p<0.01$, **Fig. 2e**) compared to the *Msr1*$^{-/-}$ mice.
215 Next, we characterized the livers of HFD-WT and HFD- *Msr1*$^{-/-}$ mice by high-throughput RNA
216 sequencing analysis. The analysis revealed 728 differentially expressed genes (adjusted p-
217 value<0.05, **Fig. S3c**, **Table S2**). Gene Ontology analysis of differentially expressed genes
218 highlighted an enrichment for genes correlating to biological processes including "immune
219 system process", "innate immune response", "phagocytosis" and "lipid metabolic process" (**Fig.**
220 **2f**, **Fig.S3d**). *Msr1*$^{-/-}$ mice displayed a reduced hepatic transcript expression of inflammatory
221 cytokines (including *Axl*, *Ccl6*, *Il1b*, *Spp1*), pro-inflammatory immune cell markers (*Ccr5*, *Cd14*,
222 *Cd44*, *S100a8*, *S100a9*), markers for hepatic stellate cell activation (*Sox9*, *Pdgfb*) and members
223 of the *Tnfa* signaling pathway (*Ripk3*, *Tnfaip2*, *Tnfaip8l2*) when compared with WT mice after
224 16 weeks of HFD (**Fig.2f**). Furthermore, *Msr1*$^{-/-}$ mice on HFD showed a shift in gene expression
225 associated with lipid metabolism, with genes including *Acox1*, *Acox2*, *Apoe*, *Ces1d*, *Hsd17b11*,
226 *Pla2g6* and *Ppara* increasing, and genes such as *Fabp5*, *Lpcat2*, *Lpl*, *Pla2g7* and *Pnpla3*
227 decreasing (**Fig.2f**). To further test the effect of *Msr1*-deficiency on the metabolic syndrome, we
228 measured several parameters within the serum as well as in the liver tissue. HFD-fed *Msr1*$^{-/-}$ mice
229 exhibited higher serum leptin ($p<0.05$), lower concentrations of circulating FFAs ($p<0.05$) which
230 corresponded to reduced hepatic triglycerides (TGs, $p<0.01$) and enhanced lipid utilization
231 measured by approximately 50% higher mitochondrial oxygen consumption rate in the liver
232 compared to HFD-fed WT mice ($p<0.001$) (*22*), while circulating TG levels remained unchanged
233 (**Fig. 2g-h, Fig. S3e**). Moreover, the absence of *Msr1* improved glucose uptake from blood in
234 obese mice ($p<0.01$, **Fig. S3f**). Taken together, these results demonstrate that *Msr1* deficiency

235 increases the body weight but protects against features of the metabolic syndrome, including
236 liver inflammation and fibrosis, while modulating hepatic lipid metabolism.
237
238 *Msr1 deficiency prevents formation of pro-inflammatory foamy macrophages in vivo*
239 Next, we asked whether the lipid-laden environment is a proximal stimulus leading to Msr1-
240 mediated inflammation in the liver and adipose tissue, which may explain the observed
241 metabolic dysfunction. In agreement with our human data, histopathological analysis of the liver
242 and adipose tissue from HFD-fed *Msr1* $^{-/-}$ mice showed no hepatic lipogranuloma and very few
243 foamy macrophages compared to their WT counterparts, demonstrated by F4/80 immunostaining
244 (**Fig. 3a**). We have recently shown that triggering of Msr1 activates the JNK signaling pathway
245 (*15*). JNK signaling is a stress-activated pathway that has been implicated in SFA-induced pro-
246 inflammatory activation of macrophages (*14*). Indeed, HFD-fed *Msr1*$^{-/-}$ mice exhibited reduced
247 hepatic JNK1/2 phosphorylation compared to the WT (**Fig. S4a**). Moreover, *Msr1*$^{-/-}$ mice
248 displayed lower Il6 and Tnfα serum levels and reduced *Tnfa* and *Il6* gene expression in the liver
249 and eWAT (**Fig. 3b-d**). Furthermore, *Msr1* deficiency impaired pro-inflammatory activation of
250 isolated adipose tissue- (ATMs) and hepatic-associated macrophages as shown by lower gene
251 transcripts of *Tnfa* and *Il6* ($p<0.01$, **Fig. 3e-g**). To extend these findings, we co-cultured either
252 primary adipocytes and hepatocytes or differentiated 3T3-L1 adipocyte-like cells and lipid-fed
253 hepatocyte-like Hepa1-6 cells indirectly with WT and *Msr1*$^{-/-}$ bone marrow-derived macrophages
254 in trans-well assays (**Fig. S4b-d**). Consistent with the *in vivo* data, *Msr1* deficiency or blocking
255 of the Msr1 receptor using a monoclonal antibody attenuated the pro-inflammatory response
256 when co-cultured with adipocytes or hepatocytes compared to WT counterpart (**Fig. S4d-f**).
257 Altogether, these results show that Msr1 mediates HFD-induced hepatic and adipose tissue
258 inflammation and facilitates macrophage activation toward a pro-inflammatory phenotype.
259
260 *Triggering of Msr1 by lipids induces JNK-mediated pro-inflammatory activation of macrophages*
261 We next investigated the underlying mechanism of Msr1-mediated lipid-induced inflammation.
262 We reasoned that Msr1 is directly responsible for lipid uptake in macrophages, leading to an
263 inflammatory response independent from other cell types. In this regard, we measured the uptake
264 of SFA (palmitic acid) and non-SFA (oleic acid) in either hepatic macrophages or bone marrow-
265 derived macrophages (BMDMs) by quantifying Oil-red-O staining using confocal microscopy

266 (**Fig. 4a-c**). The analysis revealed that Msr1 facilitates the uptake of both SFA as well as non-
267 SFA but only SFA induced enhanced levels of *Tnfa* and *Il6* transcripts and phosphorylation of
268 JNK signaling in WT macrophages (**Fig. 4d,e, Fig. S5a-c)**. Furthermore, blocking of Msr1
269 receptor with a monoclonal antibody or the chemical inhibition of JNK signaling in macrophages
270 abrogated the induction of *Tnfa* and *Il6* pro-inflammatory gene expression in response to SFA
271 treatment (**Fig. 4f**, **Fig.S5d**). These data indicate that SFA-induced triggering of Msr1 regulates
272 JNK-mediated pro-inflammatory activation of macrophages in the absence of
273 lipopolysaccharide.
274
275 *Therapeutic inhibition of MSR1 prevents formation of pro-inflammatory foamy macrophages*
276 To investigate the therapeutic potential of targeting MSR1 in the treatment of NAFLD, we
277 applied an antibody-based intervention using NAFLD mouse models and *ex vivo* human liver
278 slices. WT mice were fed a HFD for 12 weeks and were administered two doses of monoclonal
279 rat anti-mouse Msr1 antibody (n=3 animals) or isotype-matched IgG control (n=4 animals) at
280 week 10 and 11 by intravenous injection (**Fig. 5a**). Histological assessment by F4/80 staining
281 showed a reduction in foamy macrophages and lipogranulomas in the livers of mice treated with
282 anti-Msr1compared to the IgG control (**Fig. 5b**). Digital quantification of the F4/80 stainings
283 indicated a significant reduction in surface area positivity of hepatic macrophages in the anti-
284 Msr1 treated animals ($p<0.05$, **Fig.5c**). Furthermore, treated animals showed reduced expression
285 of *Tnfa* transcript in liver samples and isolated hepatic macrophages ($p<0.05$, **Fig.5d**).
286 To further investigate whether inhibition of MSR1 prevents the formation of foamy macrophages
287 in humans, we collected human liver slices with normal morphology from two different patients
288 (2 biological replicates per condition for each patient sample). The samples were incubated with
289 a polyclonal rabbit anti-human MSR1 antibody prior to culturing them with a mixture of OA
290 (2mM) and PA (1mM) in combination with anti-MSR1 antibody for a total duration of 16h
291 (**Fig.5e**). Treatment with the antibody reduced the accumulation of lipids within the macrophages
292 as shown by the CD68 immunohistochemical staining (**Fig.5f**). Digital quantification of the
293 CD68 staining showed a significant reduction in surface area positivity of Kupffer cells upon
294 antibody treatment in both patient samples as compared to the non-treated condition ($p<0.001$,
295 four areas quantified per biological replicate, **Fig.5g**). Moreover, lipid loading induced the
296 release of TNFα into the cell culture medium as compared to the bovine serum albumin (BSA)

297 control in both patient samples ($p<0.0001$, two technical replicates per biological replicate),
298 which was significantly reduced upon treatment with anti-MSR1 antibody ($p<0.01$)(**Fig.5h**).
299 Overall, our *in vivo* and *ex vivo* results show that therapeutic inhibition of MSR1 prevents the
300 formation of foamy macrophages and the release of TNFα.
301
302 Relevance of polymorphisms in *MSR1* region to NAFLD and metabolic traits
303 Next, we asked whether genetic variants in MSR1 are associated with susceptibility to NAFLD
304 and if there is an association with transcriptional regulatory mechanisms controlling *MSR1*
305 expression. Using previously published genomics data encompassing a cohort of 1,483 European
306 Caucasian patients with histologically proven NAFLD and 17,781 European general-population
307 controls (*23*), we identified 4 single nucleotide polymorphisms (SNPs) in or around the *MSR1*
308 locus with p-values$<5*10^{-4}$, with rs41505344 as the most significant ($p=1.64*10^{-4}$) (**Fig. 6a** and
309 **Table S3**). Quantitative trait analysis for rs41505344 in 430,101 patients enrolled in the
310 UKBiobank showed a significant correlation with serum triglycerides and aspartate transaminase
311 (AST) levels, even after adjustment for age, gender, body mass index (BMI), center, batch and
312 the first ten principal components (**Table 1**, adjusted $p=3.55*10^{-6}$ and adjusted $p=0.003$
313 respectively).
314 Our human immunohistochemistry data indicated that MSR1 is expressed in the liver on mature
315 endogenous macrophages, the Kupffer cells, rather than on infiltrating monocyte-derived
316 macrophages. To unravel transcriptional regulatory mechanisms of *MSR1*, we used publicly
317 available RNA sequencing data comparing human monocytes with differentiated macrophages,
318 which identified 1,208 differentially expressed genes, with *MSR1* mRNA expression increased in
319 the macrophage population (*24*). By motif enrichment analysis using iRegulon, we identified
320 eight differentially expressed transcription factors, upregulated in human macrophages compared
321 to monocytes, that are predicted to regulate the expression of *MSR1*: *BHLHE41*, *ETV5*, *HMGN3*,
322 *MAF*, *MITF*, *NR1H3*, *THRA* and *ZNF562* (False discover rate<0.001, **Fig.6b**, **Table s4**). To
323 verify whether these transcription factors bind any regulatory regions near the *MSR1* gene, and in
324 particular the rs41505344 SNP locus, we investigated ChIP-sequencing data for these proteins.
325 *MITF*, *MAF*, *THRA* and *NR1H3* proved to bind in the vicinity of the rs41505344 locus,
326 suggesting an indirect role for the SNP in the transcriptional regulation of *MSR1* (**Fig.6c**). Taken
327 together, these results suggest there is an increased frequency in NAFLD of variants potentially

328 affecting *MSR1* expression during monocyte-macrophage differentiation, which thereby could
329 influence features of obesity-related diseases.
330

331 **Discussion**

332 In this study, we provide evidence that MSR1 is important for the uptake of lipids in
333 macrophages leading to an inflammatory response and metabolic changes throughout the body.
334 In a setting of lipid overload, MSR1 deficiency not only led to reduced hepatic inflammation and
335 changes in hepatic lipid metabolism but it also reduced circulating fatty acids, increased lipid
336 storage in the adipose tissue and improved glucose tolerance, highlighting the importance of the
337 liver-adipose tissue axis in NAFLD and the metabolic syndrome (*25*). Our data demonstrated
338 that in NAFLD biopsies MSR1 expression was observed in tissue-resident macrophages, the
339 Kupffer cells, rather than in infiltrating monocytes, located in the portal tract (*26*). Previous
340 research showed that differentiation of human monocytes towards mature macrophages goes
341 hand-in-hand with increased expression of *MSR1* mRNA (*24*). The association between *MSR1*
342 mRNA and features of steatohepatitis (hepatocyte ballooning and lobular inflammation) as found
343 in our data, would suggest that there is an ongoing differentiation from infiltrating monocytes
344 towards macrophages during NASH. Chronic portal inflammation is a histological feature
345 correlated with advanced NAFLD in both adults and children (*27, 28*), yet it has not been
346 associated with lobular inflammation, which is a predictor of fibrosis progression in patients with
347 NAFLD (*29*). This would suggest that steatohepatitis is driven by mature tissue-resident
348 macrophages rather than infiltrating monocytes. Our results support this as *Msr1* deficiency in
349 HFD-fed mice tempered the lipid-induced inflammatory response in the liver, by reducing the
350 expression of *Axl*, *Il1b*, *S100a8/a9* and *Spp1* but also *Cd44*. Cd44 expression has been associated
351 with NASH in human and mouse, and is crucial for homing of monocytes into the damaged liver,
352 suggesting that lipid accumulation in tissue-resident macrophages via MSR1 is a trigger to
353 recruit immune cells (*30*). This is in line with previous reports where it was described that
354 Kupffer cell depletion by clodronate liposomes in mice on a choline-deficient l-amino acid-
355 defined diet for 22 weeks suppresses the infiltration of inflammatory cells, mainly monocytes,
356 into the liver (*31*). Furthermore, our results showed that the absence of Msr1 induced a change in
357 hepatic expression of genes associated with lipid metabolism, including an increase in *Ppara*,
358 reduced hepatic triglycerides with concordantly increased mitochondrial oxygen consumption

359 and ameliorated glucose tolerance in HFD-fed mice. Peroxisome proliferator–activated receptors
360 (PPAR) are nuclear receptors playing key roles in metabolic homeostasis and inflammation (*32*).
361 Selective depletion of Kupffer cells has been reported to activate Ppara signaling in hepatocytes
362 while resulting in overall reduced levels of hepatic triglycerides in mice fed a 45%-HFD for 20
363 weeks (*33*). Furthermore, hepatocyte-restricted *Ppara* deletion in mice impaired liver lipid
364 metabolism, leading to increased hepatic triglycerides and increased plasma FFAs (*34*). In
365 human adult non-cirrhotic NASH patients, the PPAR agonist lanifibranor proved to induce
366 NASH resolution and fibrosis regression after 24 weeks of treatment in a Phase 2b randomized,
367 placebo-controlled, double-blind study (*35*). Taken together, the effect of Msr1 deficiency we
368 have observed in this study on liver metabolism, triglycerides and circulating FFAs could in part
369 be explained by the changed Ppara signaling in the liver.

370 In this study, we showed that MSR1 can facilitate the uptake of SFAs, such as palmitic acid, as
371 well as non-SFAs, such as oleic acid, independent from other receptors. Yet, only SFAs could
372 induce the release of TNFα through phosphorylation of JNK in macrophages, which is in line
373 with previous reports (*12-15*). In murine methionine- and choline-deficient diet models, jnk1, but
374 not jnk2, proved to be critical for diet-induced JNK activation and the development of
375 steatohepatitis (*36*). In our *Msr1*$^{-/-}$ HFD-fed mice, we observed lower *Tnfa* expression in the liver
376 and adipose tissue as well as lower serum Tnfα levels. Furthermore, we showed that therapeutic
377 blocking of MSR1 *in vivo* or *ex vivo* using human liver slices prevented the formation of foamy
378 macrophages and reduced the release of TNFα. TNFα is of clinical relevance as serum levels
379 have been reported to be increased in obese patients and correlated with NAFLD disease activity
380 (*37, 38*). The effect of TNFα is pleiotropic as it can sensitize hepatocytes to apoptosis but it can
381 also stimulate hepatic lipid synthesis and reduce *Ppara* expression (*39-41*). Furthermore, Tnfα
382 affects glucose homeostasis in adipocytes and promotes lipolysis in cultured adipocytes (*42*).

383 Although current efforts to develop drug therapies for NAFLD primarily focus on ameliorating
384 the specific histological features of the disease (i.e. steatohepatitis or fibrosis), it is important to
385 remember that NAFLD is part of a multi-system metabolic disease state and so agents that offer
386 more broad metabolic or cardiovascular benefits would be highly attractive (*43*). Our data
387 indicate that by targeting MSR1, one would not only reduce lipid-induced inflammation in the
388 liver but also improve dyslipidemia and affect improved lipid storage in the adipocytes. In
389 addition, we demonstrate the feasibility of using targeted monoclonal antibody therapy to treat

390 NASH by reducing hepatic inflammation *in vivo* in mice and *ex vivo* in human models.
391 Moreover, we found some evidence that the genetic variant rs41505344 in *MSR1* was associated
392 with serum triglycerides and ALT in a large cohort of over 400,000 patients. Though the SNP in
393 *MSR1* was not strongly associated with susceptibility to NAFLD, we found that several
394 transcription factors regulating the expression of *MSR1* bound in the locus of this SNP. This
395 would suggest that rs41505344 could influence the expression of *MSR1* during macrophage
396 differentiation/maturation and hence effect levels of serum triglycerides and ALT.

397 There are several limitations to this study. Although we have used large cohorts of adult patients,
398 we do not know if we do not know if the results would be similar in paediatric NAFLD. In
399 addition, we did not provide any functional proof for the role of rs41505344 in a setting of lipid-
400 overload. To investigate the effect rs41505344 on *MSR1* expression and features of the metabolic
401 syndrome, a knock-in mouse model challenged with a long-term diet could help to provide
402 answers. Moreover, in this current study we used a global knock-out mouse model and focused
403 on the early phases of NAFLD by using a relative short-term diet of 16 weeks. To further
404 investigate the liver-adipose tissue axis, a Kupffer cell-specific *Msr1* knock-out or a conditional
405 *Msr1* knock-out mouse model could be used. In this study, we focused on MSR1 in a setting of
406 lipid overload, yet other macrophage scavenger receptors have been reported to play a role
407 during the metabolic syndrome. TREM2 has been described to induce liver fibrosis and regulate
408 adipose tissue homeostasis (*19, 20*), while soluble CD163 has been associated with adipose
409 tissue insulin resistance, circulating FFAs and hepatic steatosis (*44*). Although, our RNA
410 sequencing data of HFD-fed *Msr1-/-* mice showed no differential expression for these receptors,
411 this does not necessarily exclude synergy in function or pathway signaling between these
412 receptors.

413 This study showed that the scavenger receptor MSR1, as part of the innate immune system, is a
414 critical sensor for lipid homeostasis, highlighting the importance of the liver-adipose tissue axis.
415 With the prevalence of obesity increasing globally, it is crucial that we understand how our
416 immune system reacts when challenged with over-nutrition. Understanding and therapeutically
417 influencing macrophage immunometabolism, could help us treat features of the metabolic
418 syndrome, such as dyslipidemia, NAFLD and type II diabetes.

419

420 **Materials and Methods**

421 **Study design**

422 A total of 170 adult NAFLD liver biopsies were processed for transcriptomic analysis and MSR1
423 protein expression was assessed in 14 liver and 31 adipose tissue biopsies, and correlated with
424 clinicopathological features. To functionally validate our findings, *Msr1-/-* and WT mice were
425 submitted to a high fat and cholesterol diet for 16 weeks. The Msr1 receptor and down-stream
426 signaling targets were inhibited *in vitro* using isolated mouse primary macrophages and bone
427 marrow-derived macrophages, challenged with lipids. Therapeutic intervention with monoclonal
428 antibody against MSR1 was performed in WT mice on a 12 week high fat and cholesterol diet,
429 and in lipid loaded *ex vivo* human liver slices. To assess susceptibility with NAFLD and the
430 metabolic syndrome, GWAS analysis was performed using previously published data including
431 1,483 European NAFLD cases and 17,781 European general-population controls (*23*). Results
432 were replicated using clinical data from 430,101 participants of the UKBiobank. Publicly
433 available RNA sequencing data was used to investigate the association between SNPs and
434 transcription factors regulating *MSR1* expression when differentiating human monocytes towards
435 macrophages.

436 **Patient selection**

437 Cases were derived from the European NAFLD Registry (*45*). For the histopathological and
438 nanoString® study, 215 liver and adipose tissue samples from Caucasian patients were included.
439 184 formalin-fixed paraffin-embedded (FFPE) or frozen liver biopsies samples were obtained
440 from patients diagnosed with histological proven NAFLD at the Freeman Hospital, Newcastle
441 Hospitals NHS Foundation Trust, Newcastle-upon-Tyne, UK and at the Pitié-Salpêtrière
442 Hospital, Paris, France. In addition, 20 FFPE subcutaneous adipose tissue samples and 11
443 matching omental adipose tissue samples were obtained from obese patients with or without
444 NAFLD, diagnosed and treated at the Pitié-Salpêtrière Hospital, Paris, France (Table S5). For the
445 Genome Wide Association Study, 1,483 patients with histological proven NAFLD recruited at
446 different European centers were included as previously described (*23*). All liver tissue samples
447 for the histopathological and nanoString® study were centrally scored according to the
448 semiquantitative NASH-CRN Scoring System by an expert liver pathologist (DT) (*18*). Fibrosis
449 was staged from F0 through to F4 (cirrhosis). Alternate diagnoses and etiologies such as

excessive alcohol intake, viral hepatitis, autoimmune liver diseases and steatogenic medication use were excluded. Viable human normal liver tissue for the *ex vivo* slices was obtained after resection from two adult patients treated at the University Hospitals Leuven, Leuven, Belgium. Samples were assessed by an expert liver pathologist (TR). This study was approved by the local or national relevant Ethical Committees of each in the participating center.

nanoString

mRNA was isolated from 170 liver biopsy samples (FFPE and frozen). AllPrep DNA/RNA Micro kit (Qiagen) was used for the frozen samples, the High Pure FFPET RNA Isolation Kit (06650775001, Life Science Roche) for the FFPE biopsies. Custom-made assay panels were run on the nanoString® nCounter analysis system (nanoString®). The nSolver 3.0 software (nanoString®) was used for positive and negative control probe validation and the data were normalized to three housekeeping genes (*RPL19*, *SRSF4* and *YWHAZ*).

Animals

Msr1-/- C57BL/6 mice were kindly provided by Prof. Siamon Gordon, University of Oxford. All mice were maintained under specific pathogen free conditions and experiments were approved by the Institutional Animal Care and Use Committee and with a project license of the UK Home office. Mice had free access to water and were fed either standard chow (n=10, 5 WT and 5 *Msr1-/-*) or high-fat and high-cholesterol diets (n=10, 5 WT and 5 *Msr1-/-*; 45%-HFD; 820263, Special Diet Services) ad libitum. Body weight was measured weekly during the feeding period and compared with liver weight and visceral fat mass after the animals were sacrificed. For the therapeutic intervention study, WT mice were put on a high-fat and high-cholesterol diet (45%-HFD; 820263, Special Diet Services) for 12 weeks and treated with monoclonal rat anti-mouse Msr1 antibody (n=3 animals, (MAB1797-SP) R&Dsystems) or rat IgG control (n=4 animals, (MAB0061) R&D systems) at week 10 and 11 by intravenous injection (0.25 mg of Msr1 antibody or corresponding IgG control for each animal).

Statistical analysis

Data were tested for normality using the Kolmogorov-Smirnov or the Shapiro-Wilk normality test using GraphPad Prism 8.0.1 (GraphPad Software Inc.). Unpaired Student's t-test or Mann-Whitney U test, one way ANOVA or Kruskal-Wallis test with respectively Tuckey's or Dunn's post hoc multiple comparison test, and Spearman's rho correlation were performed using

480 GraphPad Prism 8.0.1. Data were visualized using GraphPad Prism 8.0.1. A p-value<0.05 was
481 considered significant.

482 *Additional Material and Methods can be found in the Supplementary Materials.*
483

484 **Supplementary Materials**

485 Fig. S1. Macrophage Scavenger Receptor 1 (MSR1) expression in human non-alcoholic fatty
486 liver disease (NAFLD)

487 Fig. S2. Expression of MSR1 and CD68 in human NAFLD

488 Fig. S3. Characterization HFD-fed *Msr1-/-* mice.

489 Fig. S4. Co-cultures of WT and *Msr1*$^{-/-}$ BMDMs with adipocyte- and hepatocyte-like cells.

490 Fig. S5. Msr1 regulates lipid-induced pro-inflammatory activation of macrophages through JNK
491 signaling.

492 Table S1. Demographics patient cohort used for nanoString analysis.

493 Table S2. Differentially expressed genes comparing HFD-fed *Msr1-/-* with WT mice using RNA
494 sequencing.

495 Table S3. Top *MSR1* SNPs in GWAS analysis NAFLD Case (n=1,483) vs control (n=17,781)
496 with p<1.0E-04

497 Table S4. iRegulon analysis identifying upregulated transcription factors binding to MSR1
498 region when comparing macrophages with monocytes.

499 Table S5. Clinical data obese patient cohort used for immunohistochemistry.

500

501 **References**:

502 1. Q. M. Anstee, H. L. Reeves, E. Kotsiliti, O. Govaere, M. Heikenwalder, From NASH to
503 HCC: current concepts and future challenges. *Nat Rev Gastroenterol Hepatol*, (2019);
504 published online EpubApr 26 (10.1038/s41575-019-0145-7).
505 2. Z. M. Younossi, A. B. Koenig, D. Abdelatif, Y. Fazel, L. Henry, M. Wymer, Global
506 epidemiology of nonalcoholic fatty liver disease-Meta-analytic assessment of prevalence,
507 incidence, and outcomes. *Hepatology* **64**, 73-84 (2016); published online EpubJul
508 (10.1002/hep.28431).
509 3. O. Govaere, S. Cockell, D. Tiniakos, R. Queen, R. Younes, M. Vacca, L. Alexander, F.
510 Ravaioli, J. Palmer, S. Petta, J. Boursier, C. Rosso, K. Johnson, K. Wonders, C. P. Day,
511 M. Ekstedt, M. Oresic, R. Darlay, H. J. Cordell, F. Marra, A. Vidal-Puig, P. Bedossa, J.
512 M. Schattenberg, K. Clement, M. Allison, E. Bugianesi, V. Ratziu, A. K. Daly, Q. M.
513 Anstee, Transcriptomic profiling across the nonalcoholic fatty liver disease spectrum
514 reveals gene signatures for steatohepatitis and fibrosis. *Sci Transl Med* **12**, (2020);
515 published online EpubDec 2 (10.1126/scitranslmed.aba4448).
516 4. A. Leroux, G. Ferrere, V. Godie, F. Cailleux, M. L. Renoud, F. Gaudin, S. Naveau, S.
517 Prevot, S. Makhzami, G. Perlemuter, A. M. Cassard-Doulcier, Toxic lipids stored by
518 Kupffer cells correlates with their pro-inflammatory phenotype at an early stage of
519 steatohepatitis. *J Hepatol* **57**, 141-149 (2012); published online EpubJul
520 (10.1016/j.jhep.2012.02.028).
521 5. O. Krenkel, T. Puengel, O. Govaere, A. T. Abdallah, J. C. Mossanen, M. Kohlhepp, A.
522 Liepelt, E. Lefebvre, T. Luedde, C. Hellerbrand, R. Weiskirchen, T. Longerich, I. G.
523 Costa, Q. M. Anstee, C. Trautwein, F. Tacke, Therapeutic inhibition of inflammatory
524 monocyte recruitment reduces steatohepatitis and liver fibrosis. *Hepatology* **67**, 1270-
525 1283 (2018); published online EpubApr (10.1002/hep.29544).
526 6. K. Kazankov, S. M. D. Jorgensen, K. L. Thomsen, H. J. Moller, H. Vilstrup, J. George,
527 D. Schuppan, H. Gronbaek, The role of macrophages in nonalcoholic fatty liver disease
528 and nonalcoholic steatohepatitis. *Nat Rev Gastroenterol Hepatol* **16**, 145-159 (2019);
529 published online EpubMar (10.1038/s41575-018-0082-x).
530 7. G. N. Ioannou, W. G. Haigh, D. Thorning, C. Savard, Hepatic cholesterol crystals and
531 crown-like structures distinguish NASH from simple steatosis. *J Lipid Res* **54**, 1326-1334
532 (2013); published online EpubMay (10.1194/jlr.M034876).
533 8. D. G. Tiniakos, M. B. Vos, E. M. Brunt, Nonalcoholic fatty liver disease: pathology and
534 pathogenesis. *Annu Rev Pathol* **5**, 145-171 (2010)10.1146/annurev-pathol-121808-
535 102132).
536 9. P. K. Luukkonen, S. Sadevirta, Y. Zhou, B. Kayser, A. Ali, L. Ahonen, S. Lallukka, V.
537 Pelloux, M. Gaggini, C. Jian, A. Hakkarainen, N. Lundbom, H. Gylling, A. Salonen, M.
538 Oresic, T. Hyotylainen, M. Orho-Melander, A. Rissanen, A. Gastaldelli, K. Clement, L.
539 Hodson, H. Yki-Jarvinen, Saturated Fat Is More Metabolically Harmful for the Human
540 Liver Than Unsaturated Fat or Simple Sugars. *Diabetes Care* **41**, 1732-1739 (2018);
541 published online EpubAug (10.2337/dc18-0071).
542 10. P. K. Luukkonen, Y. Zhou, S. Sadevirta, M. Leivonen, J. Arola, M. Oresic, T.
543 Hyotylainen, H. Yki-Jarvinen, Hepatic ceramides dissociate steatosis and insulin
544 resistance in patients with non-alcoholic fatty liver disease. *J Hepatol* **64**, 1167-1175
545 (2016); published online EpubMay (10.1016/j.jhep.2016.01.002).

546 11. F. Chiappini, A. Coilly, H. Kadar, P. Gual, A. Tran, C. Desterke, D. Samuel, J. C.
547 Duclos-Vallee, D. Touboul, J. Bertrand-Michel, A. Brunelle, C. Guettier, F. Le Naour,
548 Metabolism dysregulation induces a specific lipid signature of nonalcoholic
549 steatohepatitis in patients. *Sci Rep* **7**, 46658 (2017); published online EpubApr 24
550 (10.1038/srep46658).
551 12. R. G. Holzer, E. J. Park, N. Li, H. Tran, M. Chen, C. Choi, G. Solinas, M. Karin,
552 Saturated fatty acids induce c-Src clustering within membrane subdomains, leading to
553 JNK activation. *Cell* **147**, 173-184 (2011); published online EpubSep 30
554 (10.1016/j.cell.2011.08.034).
555 13. C. Shrestha, T. Ito, K. Kawahara, B. Shrestha, M. Yamakuchi, T. Hashiguchi, I.
556 Maruyama, Saturated fatty acid palmitate induces extracellular release of histone H3: a
557 possible mechanistic basis for high-fat diet-induced inflammation and thrombosis.
558 *Biochem Biophys Res Commun* **437**, 573-578 (2013); published online EpubAug 9
559 (10.1016/j.bbrc.2013.06.117).
560 14. G. I. Lancaster, K. G. Langley, N. A. Berglund, H. L. Kammoun, S. Reibe, E. Estevez, J.
561 Weir, N. A. Mellett, G. Pernes, J. R. W. Conway, M. K. S. Lee, P. Timpson, A. J.
562 Murphy, S. L. Masters, S. Gerondakis, N. Bartonicek, D. C. Kaczorowski, M. E. Dinger,
563 P. J. Meikle, P. J. Bond, M. A. Febbraio, Evidence that TLR4 Is Not a Receptor for
564 Saturated Fatty Acids but Mediates Lipid-Induced Inflammation by Reprogramming
565 Macrophage Metabolism. *Cell Metab* **27**, 1096-1110 e1095 (2018); published online
566 EpubMay 1 (10.1016/j.cmet.2018.03.014).
567 15. M. Guo, A. Hartlova, M. Gierlinski, A. Prescott, J. Castellvi, J. H. Losa, S. K. Petersen,
568 U. A. Wenzel, B. D. Dill, C. H. Emmerich, Y. C. S. Ramon, D. G. Russell, M. Trost,
569 Triggering MSR1 promotes JNK-mediated inflammation in IL-4-activated macrophages.
570 *EMBO J* **38**, (2019); published online EpubJun 3 (10.15252/embj.2018100299).
571 16. J. J. Manning-Tobin, K. J. Moore, T. A. Seimon, S. A. Bell, M. Sharuk, J. I. Alvarez-
572 Leite, M. P. de Winther, I. Tabas, M. W. Freeman, Loss of SR-A and CD36 activity
573 reduces atherosclerotic lesion complexity without abrogating foam cell formation in
574 hyperlipidemic mice. *Arterioscler Thromb Vasc Biol* **29**, 19-26 (2009); published online
575 EpubJan (10.1161/ATVBAHA.108.176644).
576 17. M. Van Eck, M. P. J. De Winther, N. Herijgers, L. M. Havekes, M. H. Hofker, P. H. E.
577 Groot, T. J. C. Van Berkel, Effect of human scavenger receptor class A overexpression in
578 bone marrow-derived cells on cholesterol levels and atherosclerosis in ApoE-deficient
579 mice. *Arterioscl Throm Vas* **20**, 2600-2606 (2000); published online EpubDec (Doi
580 10.1161/01.Atv.20.12.2600).
581 18. D. E. Kleiner, E. M. Brunt, M. Van Natta, C. Behling, M. J. Contos, O. W. Cummings, L.
582 D. Ferrell, Y. C. Liu, M. S. Torbenson, A. Unalp-Arida, M. Yeh, A. J. McCullough, A. J.
583 Sanyal, N. Nonalcoholic Steatohepatitis Clinical Research, Design and validation of a
584 histological scoring system for nonalcoholic fatty liver disease. *Hepatology* **41**, 1313-
585 1321 (2005); published online EpubJun (10.1002/hep.20701).
586 19. P. Ramachandran, R. Dobie, J. R. Wilson-Kanamori, E. F. Dora, B. E. P. Henderson, N.
587 T. Luu, J. R. Portman, K. P. Matchett, M. Brice, J. A. Marwick, R. S. Taylor, M.
588 Efremova, R. Vento-Tormo, N. O. Carragher, T. J. Kendall, J. A. Fallowfield, E. M.
589 Harrison, D. J. Mole, S. J. Wigmore, P. N. Newsome, C. J. Weston, J. P. Iredale, F.
590 Tacke, J. W. Pollard, C. P. Ponting, J. C. Marioni, S. A. Teichmann, N. C. Henderson,

591 Resolving the fibrotic niche of human liver cirrhosis at single-cell level. *Nature* **575**, 512-
592 518 (2019); published online EpubNov (10.1038/s41586-019-1631-3).
593 20. D. A. Jaitin, L. Adlung, C. A. Thaiss, A. Weiner, B. Li, H. Descamps, P. Lundgren, C.
594 Bleriot, Z. Liu, A. Deczkowska, H. Keren-Shaul, E. David, N. Zmora, S. M. Eldar, N.
595 Lubezky, O. Shibolet, D. A. Hill, M. A. Lazar, M. Colonna, F. Ginhoux, H. Shapiro, E.
596 Elinav, I. Amit, Lipid-Associated Macrophages Control Metabolic Homeostasis in a
597 Trem2-Dependent Manner. *Cell* **178**, 686-698 e614 (2019); published online EpubJul 25
598 (10.1016/j.cell.2019.05.054).
599 21. G. Farrell, J. M. Schattenberg, I. Leclercq, M. M. Yeh, R. Goldin, N. Teoh, D. Schuppan,
600 Mouse Models of Nonalcoholic Steatohepatitis: Toward Optimization of Their Relevance
601 to Human Nonalcoholic Steatohepatitis. *Hepatology* **69**, 2241-2257 (2019); published
602 online EpubMay (10.1002/hep.30333).
603 22. N. Martinez-Lopez, M. Garcia-Macia, S. Sahu, D. Athonvarangkul, E. Liebling, P.
604 Merlo, F. Cecconi, G. J. Schwartz, R. Singh, Autophagy in the CNS and Periphery
605 Coordinate Lipophagy and Lipolysis in the Brown Adipose Tissue and Liver. *Cell Metab*
606 **23**, 113-127 (2016); published online EpubJan 12 (10.1016/j.cmet.2015.10.008).
607 23. Q. M. Anstee, R. Darlay, S. Cockell, M. Meroni, O. Govaere, D. Tiniakos, A. D. Burt, P.
608 Bedossa, J. Palmer, Y. L. Liu, G. P. Aithal, M. Allison, H. Yki-Jarvinen, M. Vacca, J. F.
609 Dufour, P. Invernizzi, D. Prati, M. Ekstedt, S. Kechagias, S. Francque, S. Petta, E.
610 Bugianesi, K. Clement, V. Ratziu, J. M. Schattenberg, L. Valenti, C. P. Day, H. J.
611 Cordell, A. K. Daly, E. P. C. Investigators, Genome-wide association study of non-
612 alcoholic fatty liver and steatohepatitis in a histologically-characterised cohort. *J Hepatol*,
613 (2020); published online EpubApr 13 (10.1016/j.jhep.2020.04.003).
614 24. C. Dong, G. Zhao, M. Zhong, Y. Yue, L. Wu, S. Xiong, RNA sequencing and
615 transcriptomal analysis of human monocyte to macrophage differentiation. *Gene* **519**,
616 279-287 (2013); published online EpubMay 1 (10.1016/j.gene.2013.02.015).
617 25. A. Gastaldelli, K. Cusi, From NASH to diabetes and from diabetes to NASH:
618 Mechanisms and treatment options. *JHEP Rep* **1**, 312-328 (2019); published online
619 EpubOct (10.1016/j.jhepr.2019.07.002).
620 26. O. Govaere, S. Cockell, M. Van Haele, J. Wouters, W. Van Delm, K. Van den Eynde, A.
621 Bianchi, R. van Eijsden, W. Van Steenbergen, D. Monbaliu, F. Nevens, T. Roskams,
622 High-throughput sequencing identifies aetiology-dependent differences in ductular
623 reaction in human chronic liver disease. *J Pathol* **248**, 66-76 (2019); published online
624 EpubMay (10.1002/path.5228).
625 27. E. M. Brunt, D. E. Kleiner, L. A. Wilson, A. Unalp, C. E. Behling, J. E. Lavine, B. A.
626 Neuschwander-Tetri, N. C. R. N. l. o. m. o. t. N. S. C. R. N. c. b. f. i. t. Appendix, Portal
627 chronic inflammation in nonalcoholic fatty liver disease (NAFLD): a histologic marker of
628 advanced NAFLD-Clinicopathologic correlations from the nonalcoholic steatohepatitis
629 clinical research network. *Hepatology* **49**, 809-820 (2009); published online EpubMar
630 (10.1002/hep.22724).
631 28. J. P. Mann, R. De Vito, A. Mosca, A. Alisi, M. J. Armstrong, M. Raponi, U. Baumann,
632 V. Nobili, Portal inflammation is independently associated with fibrosis and metabolic
633 syndrome in pediatric nonalcoholic fatty liver disease. *Hepatology* **63**, 745-753 (2016);
634 published online EpubMar (10.1002/hep.28374).

29. C. K. Argo, P. G. Northup, A. M. Al-Osaimi, S. H. Caldwell, Systematic review of risk factors for fibrosis progression in non-alcoholic steatohepatitis. *J Hepatol* **51**, 371-379 (2009); published online EpubAug (10.1016/j.jhep.2009.03.019).
30. S. Patouraux, D. Rousseau, S. Bonnafous, C. Lebeaupin, C. Luci, C. M. Canivet, A. S. Schneck, A. Bertola, M. C. Saint-Paul, A. Iannelli, J. Gugenheim, R. Anty, A. Tran, B. Bailly-Maitre, P. Gual, CD44 is a key player in non-alcoholic steatohepatitis. *J Hepatol* **67**, 328-338 (2017); published online EpubAug (10.1016/j.jhep.2017.03.003).
31. K. Miura, L. Yang, N. van Rooijen, H. Ohnishi, E. Seki, Hepatic recruitment of macrophages promotes nonalcoholic steatohepatitis through CCR2. *Am J Physiol Gastrointest Liver Physiol* **302**, G1310-1321 (2012); published online EpubJun 1 (10.1152/ajpgi.00365.2011).
32. S. Francque, G. Szabo, M. F. Abdelmalek, C. D. Byrne, K. Cusi, J. F. Dufour, M. Roden, F. Sacks, F. Tacke, Nonalcoholic steatohepatitis: the role of peroxisome proliferator-activated receptors. *Nat Rev Gastroenterol Hepatol* **18**, 24-39 (2021); published online EpubJan (10.1038/s41575-020-00366-5).
33. R. Stienstra, F. Saudale, C. Duval, S. Keshtkar, J. E. Groener, N. van Rooijen, B. Staels, S. Kersten, M. Muller, Kupffer cells promote hepatic steatosis via interleukin-1beta-dependent suppression of peroxisome proliferator-activated receptor alpha activity. *Hepatology* **51**, 511-522 (2010); published online EpubFeb (10.1002/hep.23337).
34. A. Montagner, A. Polizzi, E. Fouche, S. Ducheix, Y. Lippi, F. Lasserre, V. Barquissau, M. Regnier, C. Lukowicz, F. Benhamed, A. Iroz, J. Bertrand-Michel, T. Al Saati, P. Cano, L. Mselli-Lakhal, G. Mithieux, F. Rajas, S. Lagarrigue, T. Pineau, N. Loiseau, C. Postic, D. Langin, W. Wahli, H. Guillou, Liver PPARalpha is crucial for whole-body fatty acid homeostasis and is protective against NAFLD. *Gut* **65**, 1202-1214 (2016); published online EpubJul (10.1136/gutjnl-2015-310798).
35. S. M. Francque, P. Bedossa, V. Ratziu, Q. M. Anstee, E. Bugianesi, A. J. Sanyal, R. Loomba, S. A. Harrison, R. I. Balabanska, L. Mateva, N. Lanthier, N. Alkhouri, C. Moreno, J. M. Schattenberg, D. Stefanova-Petrova, L. Vonghia, R. Rouzier, M. Guillaume, V. Leroy, M. Romero-Gomez, A. D. Hodge, P. Huot-Marchand, N. Sabin, M. Baudin, J. L. Abitbol, P. Broqua, J. L. Junien, M. F. Abdelmalek, THE PANPPAR AGONIST LANIFIBRANOR INDUCES BOTH RESOLUTION OF NASH AND REGRESSION OF FIBROSIS AFTER 24 WEEKS OF TREATMENT IN NON-CIRRHOTIC NASH: RESULTS OF THE NATIVE PHASE 2b TRIAL. *Hepatology* **72**, 9a-11a (2020); published online EpubNov (
36. J. M. Schattenberg, R. Singh, Y. Wang, J. H. Lefkowitch, R. M. Rigoli, P. E. Scherer, M. J. Czaja, JNK1 but not JNK2 promotes the development of steatohepatitis in mice. *Hepatology* **43**, 163-172 (2006); published online EpubJan (10.1002/hep.20999).
37. A. Katsuki, Y. Sumida, S. Murashima, K. Murata, Y. Takarada, K. Ito, M. Fujii, K. Tsuchihashi, H. Goto, K. Nakatani, Y. Yano, Serum levels of tumor necrosis factor-alpha are increased in obese patients with noninsulin-dependent diabetes mellitus. *J Clin Endocrinol Metab* **83**, 859-862 (1998); published online EpubMar (10.1210/jcem.83.3.4618).
38. M. Manco, M. Marcellini, G. Giannone, V. Nobili, Correlation of serum TNF-alpha levels and histologic liver injury scores in pediatric nonalcoholic fatty liver disease. *Am J Clin Pathol* **127**, 954-960 (2007); published online EpubJun (10.1309/6VJ4DWGYDU0XYJ8Q).

681 39. L. Faletti, L. Peintner, S. Neumann, S. Sandler, T. Grabinger, S. Mac Nelly, I. Merfort, C.
682 H. Huang, D. Tschaharganeh, T. W. Kang, F. Heinzmann, L. D'Artista, U. Maurer, T.
683 Brunner, S. Lowe, L. Zender, C. Borner, TNFalpha sensitizes hepatocytes to FasL-
684 induced apoptosis by NFkappaB-mediated Fas upregulation. *Cell Death Dis* **9**, 909
685 (2018); published online EpubSep 5 (10.1038/s41419-018-0935-9).
686 40. K. R. Feingold, M. Soued, I. Staprans, L. A. Gavin, M. E. Donahue, B. J. Huang, A. H.
687 Moser, R. Gulli, C. Grunfeld, Effect of tumor necrosis factor (TNF) on lipid metabolism
688 in the diabetic rat. Evidence that inhibition of adipose tissue lipoprotein lipase activity is
689 not required for TNF-induced hyperlipidemia. *J Clin Invest* **83**, 1116-1121 (1989);
690 published online EpubApr (10.1172/JCI113991).
691 41. K. Beier, A. Volkl, H. D. Fahimi, TNF-alpha downregulates the peroxisome proliferator
692 activated receptor-alpha and the mRNAs encoding peroxisomal proteins in rat liver.
693 *FEBS Lett* **412**, 385-387 (1997); published online EpubJul 28 (10.1016/s0014-
694 5793(97)00805-3).
695 42. W. P. Cawthorn, J. K. Sethi, TNF-alpha and adipocyte biology. *FEBS Lett* **582**, 117-131
696 (2008); published online EpubJan 9 (10.1016/j.febslet.2007.11.051).
697 43. L. A. Adams, Q. M. Anstee, H. Tilg, G. Targher, Non-alcoholic fatty liver disease and its
698 relationship with cardiovascular disease and other extrahepatic diseases. *Gut* **66**, 1138-
699 1153 (2017); published online EpubJun (10.1136/gutjnl-2017-313884).
700 44. C. Rosso, K. Kazankov, R. Younes, S. Esmaili, M. Marietti, M. Sacco, F. Carli, M.
701 Gaggini, F. Salomone, H. J. Moller, M. L. Abate, H. Vilstrup, A. Gastaldelli, J. George,
702 H. Gronbaek, E. Bugianesi, Crosstalk between adipose tissue insulin resistance and liver
703 macrophages in non-alcoholic fatty liver disease. *J Hepatol* **71**, 1012-1021 (2019);
704 published online EpubNov (10.1016/j.jhep.2019.06.031).
705 45. T. Hardy, K. Wonders, R. Younes, G. P. Aithal, R. Aller, M. Allison, P. Bedossa, F.
706 Betsou, J. Boursier, M. J. Brosnan, A. Burt, J. Cobbold, H. Cortez-Pinto, C. P. Day, J. F.
707 Dufour, M. Ekstedt, S. Francque, S. Harrison, L. Miele, P. Nasr, G. Papatheodoridis, S.
708 Petta, D. Tiniakos, R. Torstenson, L. Valenti, A. G. Holleboom, H. Yki-Jarvinen, A.
709 Geier, M. Romero-Gomez, V. Ratziu, E. Bugianesi, J. M. Schattenberg, Q. M. Anstee, L.
710 Consortium, The European NAFLD Registry: A real-world longitudinal cohort study of
711 nonalcoholic fatty liver disease. *Contemp Clin Trials* **98**, 106175 (2020); published
712 online EpubOct 9 (10.1016/j.cct.2020.106175).
713 46. W. Huang da, B. T. Sherman, R. A. Lempicki, Systematic and integrative analysis of
714 large gene lists using DAVID bioinformatics resources. *Nat Protoc* **4**, 44-57
715 (2009)10.1038/nprot.2008.211).
716 47. W. Huang da, B. T. Sherman, R. A. Lempicki, Bioinformatics enrichment tools: paths
717 toward the comprehensive functional analysis of large gene lists. *Nucleic Acids Res* **37**, 1-
718 13 (2009); published online EpubJan (10.1093/nar/gkn923).
719 48. W. Walter, F. Sanchez-Cabo, M. Ricote, GOplot: an R package for visually combining
720 expression data with functional analysis. *Bioinformatics* **31**, 2912-2914 (2015); published
721 online EpubSep 1 (10.1093/bioinformatics/btv300).
722 49. G. Yu, L. G. Wang, Y. Han, Q. Y. He, clusterProfiler: an R package for comparing
723 biological themes among gene clusters. *OMICS* **16**, 284-287 (2012); published online
724 EpubMay (10.1089/omi.2011.0118).

725 50. X. Zhai, W. Wang, D. Dou, Y. Ma, D. Gang, Z. Jiang, B. Shi, B. Jin, A novel technique
726 to prepare a single cell suspension of isolated quiescent human hepatic stellate cells. *Sci*
727 *Rep* **9**, 12757 (2019); published online EpubSep 4 (10.1038/s41598-019-49287-7).
728 51. P. Bankhead, M. B. Loughrey, J. A. Fernandez, Y. Dombrowski, D. G. McArt, P. D.
729 Dunne, S. McQuaid, R. T. Gray, L. J. Murray, H. G. Coleman, J. A. James, M. Salto-
730 Tellez, P. W. Hamilton, QuPath: Open source software for digital pathology image
731 analysis. *Sci Rep* **7**, 16878 (2017); published online EpubDec 4 (10.1038/s41598-017-
732 17204-5).
733 52. C. Bycroft, C. Freeman, D. Petkova, G. Band, L. T. Elliott, K. Sharp, A. Motyer, D.
734 Vukcevic, O. Delaneau, J. O'Connell, A. Cortes, S. Welsh, A. Young, M. Effingham, G.
735 McVean, S. Leslie, N. Allen, P. Donnelly, J. Marchini, The UK Biobank resource with
736 deep phenotyping and genomic data. *Nature* **562**, 203-209 (2018); published online
737 EpubOct (10.1038/s41586-018-0579-z).
738 53. O. Canela-Xandri, K. Rawlik, A. Tenesa, An atlas of genetic associations in UK Biobank.
739 *Nat Genet* **50**, 1593-1599 (2018); published online EpubNov (10.1038/s41588-018-0248-
740 z).
741 54. R. Janky, A. Verfaillie, H. Imrichova, B. Van de Sande, L. Standaert, V. Christiaens, G.
742 Hulselmans, K. Herten, M. Naval Sanchez, D. Potier, D. Svetlichnyy, Z. Kalender Atak,
743 M. Fiers, J. C. Marine, S. Aerts, iRegulon: from a gene list to a gene regulatory network
744 using large motif and track collections. *PLoS Comput Biol* **10**, e1003731 (2014);
745 published online EpubJul (10.1371/journal.pcbi.1003731).
746 55. S. Oki, T. Ohta, G. Shioi, H. Hatanaka, O. Ogasawara, Y. Okuda, H. Kawaji, R. Nakaki,
747 J. Sese, C. Meno, ChIP-Atlas: a data-mining suite powered by full integration of public
748 ChIP-seq data. *EMBO Rep* **19**, (2018); published online EpubDec
749 (10.15252/embr.201846255).
750

751

752

753 **Acknowledgments:** The authors would like to thank the Newcastle Bioimaging Unit, the
754 Newcastle University Genomics Core Facility, the Newcastle NanoString Core Facility and the
755 Newcastle Molecular Pathology Node Proximity Laboratory for their technical support.

756 **Funding**: This study has been supported by the EPoS (Elucidating Pathways of Steatohepatitis)
757 consortium funded by the Horizon 2020 Framework Program of the European Union under
758 Grant Agreement 634413 and the Newcastle NIHR Biomedical Research Centre (to QMA), the
759 Newcastle University start-up funding and the Wellcome Trust Investigator Award
760 (215542/Z/19/Z) (to MT), Knut och Alice Wallenberg Foundation Wallenberg Centre for
761 molecular and translational medicine, University of Gothenburg, Sweden and Åke Wirbergs
762 Research funding #M18-0121 (to AH), Cancerfonfen # 19 0352 Pj (2020-2022) (to AH), the
763 Belgian Federal Science Policy Office (Interuniversity Attraction Poles Program) grant Network
764 P7/83-HEPRO2 (to TR) and Rosetrees Trust (to NML).

765 **Author contributions:** OG and AH conceived the study. Study design, manuscript drafting and
766 funding: AH, OG, MT and QMA. Manuscript preparation: AH, OG, SKP, MT, QMA. *In vivo*
767 experiments: AH, SKP, OBG and NML. *In vitro* experiments: AH, OG and SKP. Human *ex vivo*
768 experiments: OG, MVH, TR. Histopathology: OG, MVH, TR and DT. Nanostring analysis: OG.
769 Bioinformatics: OG and JW. GWAS analysis: RD, HJC, AKD. eQTL UKBiobank data: RMM,
770 OJ, SR. All authors contributed to data collection and interpretation, and critically revised the
771 manuscript for intellectual content.

772 **Competing interests**: Quentin M. Anstee reports grants from European Commission during the
773 conduct of the study; other grants from Abbvie, Allergan/Tobira, AstraZeneca,
774 GlaxoSmithKline, Glympse Bio, Novartis Pharma AG, Pfizer Ltd., Vertex; consultancy for
775 89Bio, Abbott Laboratories, Acuitas Medical, Allergan/Tobira, Altimmune, AstraZeneca,
776 Axcella, Blade, BMS, BNN Cardio, Celgene, Cirius, CymaBay, EcoR1, E3Bio, Eli Lilly &
777 Company Ltd., Galmed, Genentech, Genfit SA, Gilead, Grunthal, HistoIndex, Indalo, Imperial
778 Innovations, Intercept Pharma Europe Ltd., Inventiva, IQVIA, Janssen, Madrigal, MedImmune,
779 Metacrine, NewGene, NGMBio, North Sea Therapeutics, Novartis, Novo Nordisk A/S, PathAI,
780 Pfizer Ltd., Poxel, ProSciento, Raptor Pharma, Servier, Terns, Viking Therapeutics; speaker for
781 Abbott Laboratories, Allergan/Tobira, BMS, Clinical Care Options, Falk, Fishawack, Genfit SA,
782 Gilead, Integritas Communications, Kenes, MedScape; and royalties from Elsevier Ltd

783 (Davidson's Principles & Practice of Medicine textbook). Dina Tiniakos reports consultation
784 fees from Intercept Pharmaceuticals Inc, Allergan, Cirius Therapeutics and an educational grant
785 from Histoindex Pte Ltd. Guruprasad P. Aithal reports institutional consultancy income outside
786 the scope of this study from GSK and Pfizer. Michael Allison reports consultancy/advisory with
787 MedImmune/Astra Zeneca, E3Bio, honoraria from Intercept, Grant support from GSK, Takeda.
788 Mattias Ekstedt reports personal fees from AbbVie, AstraZeneca, Albireo, Diapharma, Gilead
789 and non-financial support from Echosens (through LITMUS IMI project). Jean-Francois Dufour
790 reports advisory committees with AbbVie, Bayer, BMS, Falk, Genfit, Genkyotex, Gilead
791 Science, HepaRegenix, Intercept, Lilly, Merck, Novartis and speaking and teaching with Bayer,
792 BMS, Intercept, Genfit, Gilead Science, Novartis. Karine Clement has no personal honoraria but
793 has consultancy and scientific collaboration activity for LNC therapeutics, Confotherapeutics
794 and Danone Research. Jörn M. Schattenberg reports grants from Gilead and Boehringer
795 Ingelheim and fees from Gilead, Boehringer Ingelheim, Galmed, Genfit, Intercept, Novartis,
796 Pfizer and AbbVie outside the submitted work. Elisabetta Bugianesi reports advisory/consulting
797 for BMS, Genfit SA, Gilead, Intercept, Novartis. Melker Göransson is employed by
798 AstraZeneca. All other authors declare that they have no competing interests.

799 **Data and materials availability**:

800 To review GEO accession GSE163471:
801 Go to https://www.ncbi.nlm.nih.gov/geo/query/acc.cgi?acc=GSE163471
802

Figures

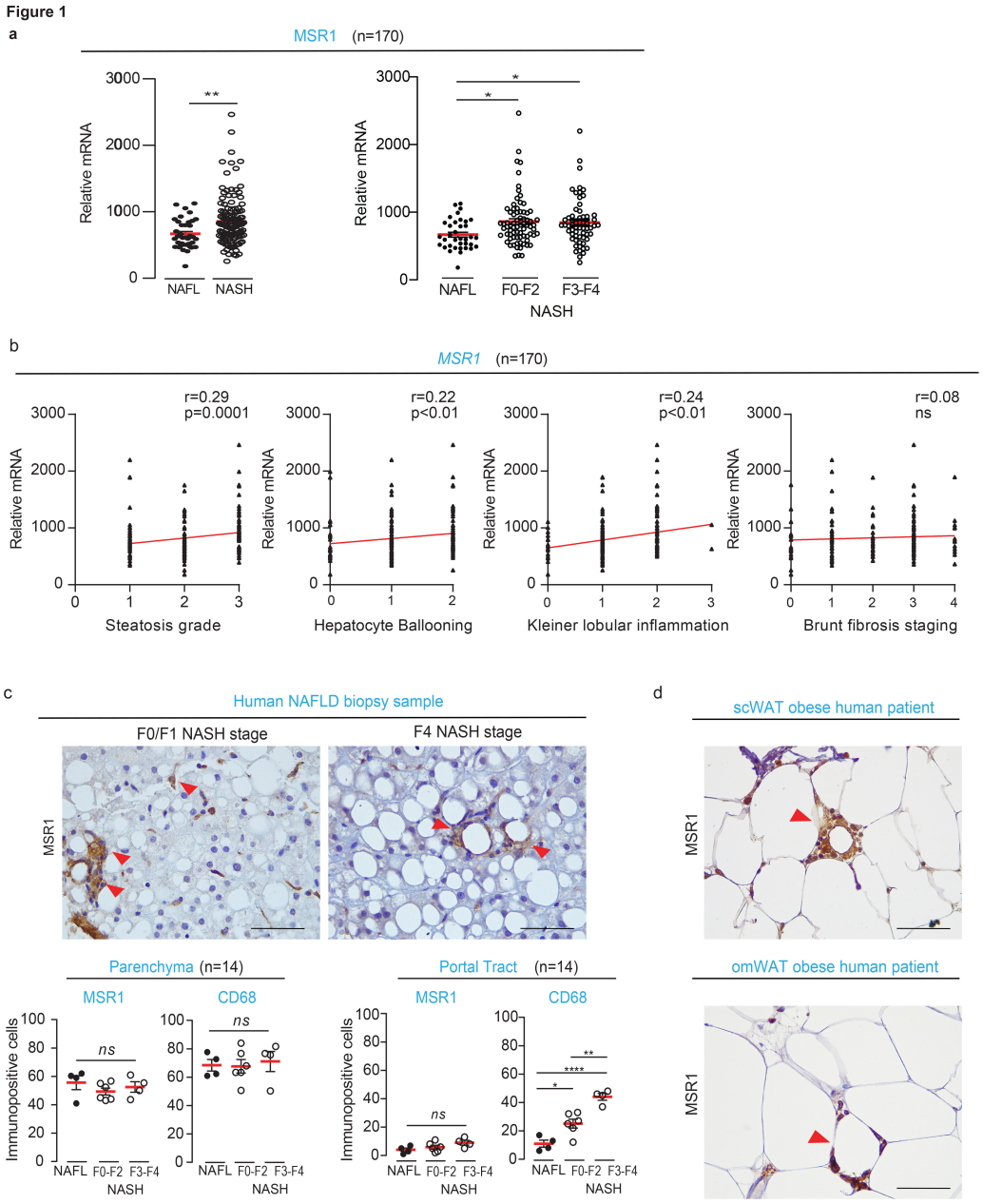

Fig. 1. Macrophage Scavenger Receptor 1 (MSR1) expression in human non-alcoholic fatty liver disease (NAFLD) correlates with steatosis and steatohepatitis. (**a**) mRNA levels of *MSR1* in a cohort of 170 histological proven NAFLD samples covering the different stages of the disease (NAFL non-alcoholic fatty liver; NASH non-alcoholic steatohepatitis F0-4 fibrosis stage) using nanoString. Filled symbols, NAFL stage; open symbols, NASH stage. (Mann-Whitney-U test and Kruskal-Wallis with correction for multiple testing) (**b**) Correlation of *MSR1* gene expression with the steatosis, hepatocyte ballooning, lobular inflammation and fibrosis stage (Spearman correlation) (**c**) The immunohistochemical analysis of MSR1 in liver tissue of human NAFLD biopsies (n=14), red arrows indicate foamy macrophages and lipogranuloma. Histopathological quantification of MSR1 and CD68

813 immunopositive cells in the parenchyma and portal tract of human NAFLD samples with mild and advanced fibrosis
814 (NAFL n=4; NASH F0-2 n=6; NASH F3-4 n=4; one-way ANOVA or Kruskal-Wallis with correction for multiple
815 testing based on distribution). (**d**) Representative image of immunohistochemical staining for MSR1 in
816 subcutaneous and omental white adipose tissue (scWAT/omWAT) from an obese patient. Data are presented as
817 mean ± SEM (* $p<0.05$, ** $p<0.01$, *** $p<0.001$, **** $p<0.0001$, *ns:* non-significant). Scale bars 100µm.

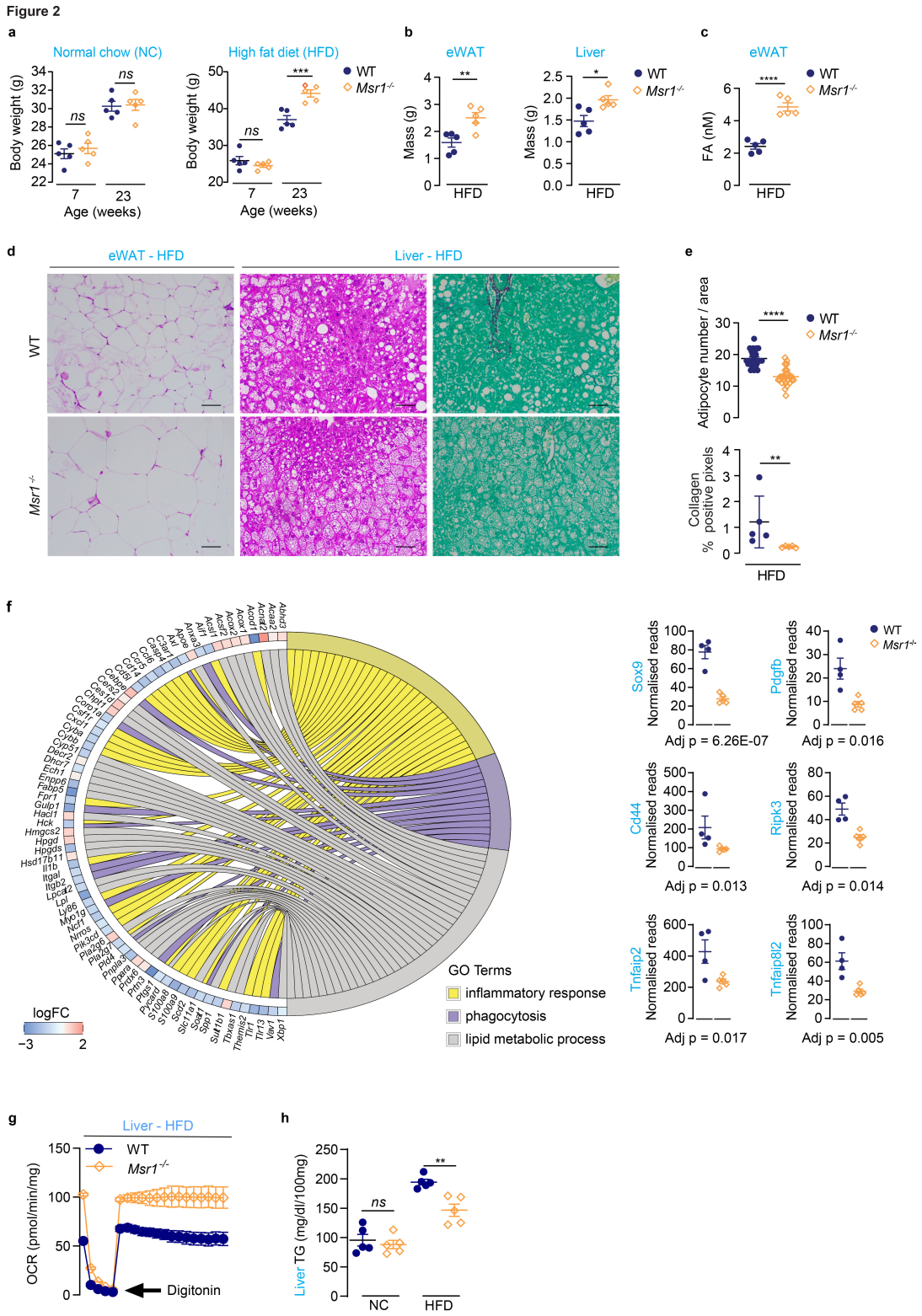

Fig. 2. Msr1 deficiency protects against HFD-associated metabolic dysregulation and liver damage. (**a**) Body weight of *Msr1*+/+ (Wild-type, WT) and *Msr1*-/- male aged-matched mice fed either with normal control chow diet

821 (NC) or high fat, high cholesterol diet (HFD) for 16 weeks (n=5 mice/experimental group) (one-way ANOVA with
822 correction for multiple testing; p-values are shown for the comparisons WT and *Msr1-/-*). (**b**) Epididymal (eWAT)
823 and liver mass of WT and *Msr1-/-* male mice fed with HFD (unpaired Student's t-test). (**c**) Quantification of fatty
824 acids in eWAT of HFD fed mice (unpaired Student's t-test). (**d**) Representative images of morphology of the eWAT
825 and liver from HFD-fed WT and *Msr1-/-* mice, as assessed by H&E staining and Picro Sirius Red Fast Green
826 staining. Scale bar 100µm. (**e**) Quantification of the adipocyte number per area and hepatic collagen deposition of
827 WT and $Msr1^{-/-}$ HFD-fed mice (n = 5 mice/experimental group; Mann-Whitney-U test). (**f**) RNA sequencing data
828 comparing Msr1-/- (n=5) with baseline WT (n=4) HFD-fed mice. Gene Ontology enrichment analysis was
829 performed for biological processes and selected differentially expressed genes were visualized. (**g**) Seahorse analysis
830 of oxygen consumption rates (OCRs) and area under curve (AUC) of HFD-WT and HFD-fed *Msr1-/-* aged-matched
831 male mice (n = 4/experimental group). (**h**) Quantification of triglycerides (TG) in liver tissue samples (n =
832 5/experimental group; one-way ANOVA with correction for multiple testing; p-values are shown for the
833 comparisons WT and *Msr1-/-*). Each symbol represent animal. Filled symbols, Msr1+/+ (WT); open symbols,
834 *Msr1-/-* mice. Data are presented as mean ± SEM (*p< 0.05, **p < 0.01, ***p < 0.001, ****p < 0.0001, ns: non-
835 significant).
836
837

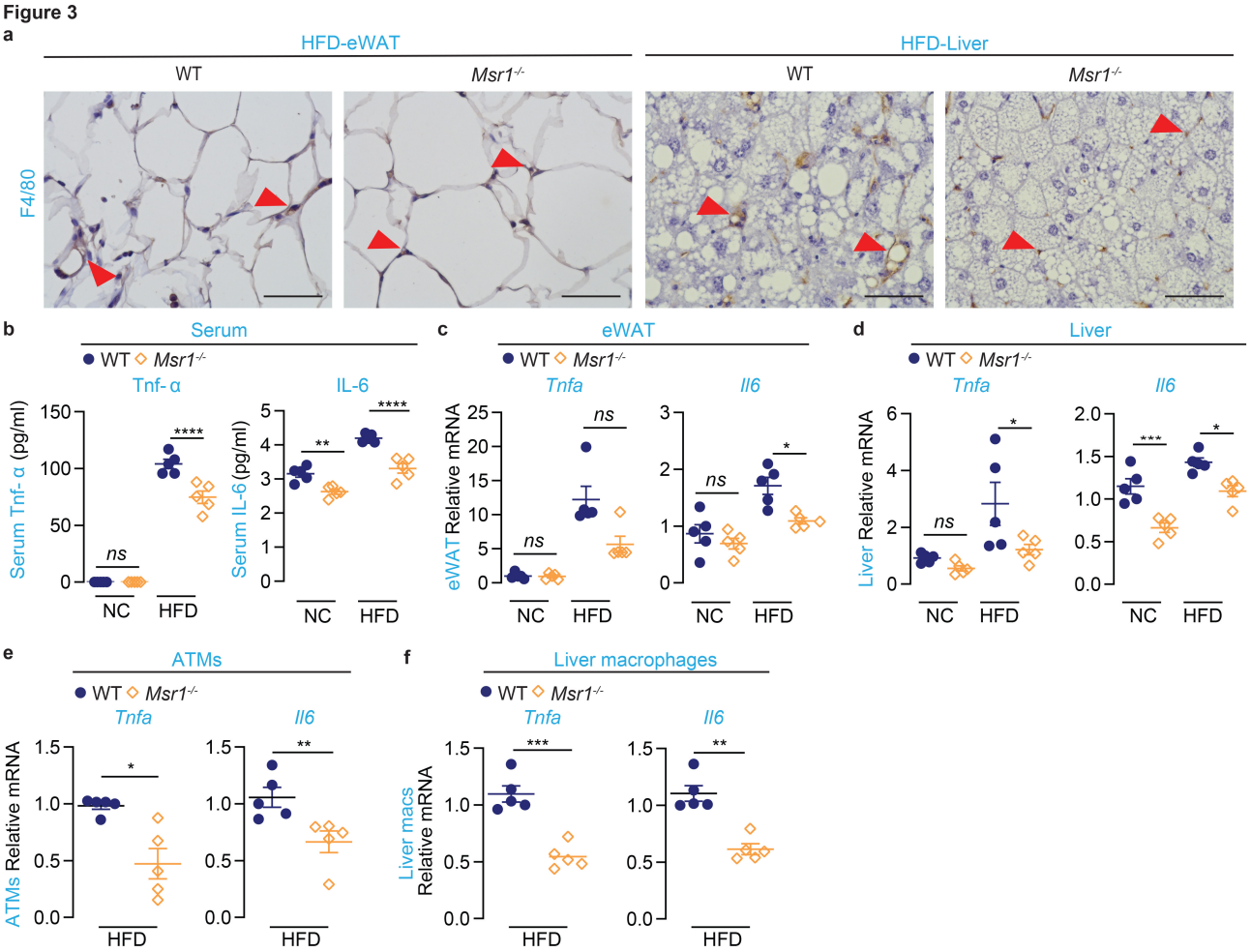

Fig. 3. Msr1 mediates HFD-induced adipose tissue and hepatic inflammation and facilitates macrophage activation toward a pro-inflammatory phenotype. (**a**) Representative images for F4/80 immunostainings in eWAT and liver tissue (scale bars 100µm) from WT and *Msr1*$^{-/-}$ HFD-fed male aged-matched mice (n=5/experimental group). Arrows indicate immunopositive cells. (**b**) Serum levels of Tnfa and Il-6 in NC- and HFD-fed mice (n=5/experimental group). **(c-d)** Quantification of mRNA levels of *Tnfa, Il6* inflammation markers in the eWAT and liver of NC- and HFD-fed mice (n=5/experimental group). (**e-f**) Real-time PCR analysis for markers of inflammation in F4/80^{+} adipose tissue (ATMs) and liver macrophages from WT and *Msr1*$^{-/-}$ HFD-fed aged-matched male mice (n=5 mice/experimental group). Each symbol represent animal. Filled symbols, *Msr1*$^{+/+}$ (WT); open symbols, *Msr1*$^{-/-}$ mice. Data are presented as mean ± SEM (unpaired Student's t-test or Mann-Whitney-U test, or one-way ANOVA or Kruskal-Wallis with correction for multiple testing based on the distribution of the data; p-values are shown for the comparisons WT and *Msr1*-/-; *p< 0.05, **p < 0.01, ***p < 0.001, ****p < 0.0001, ns: non-significant).

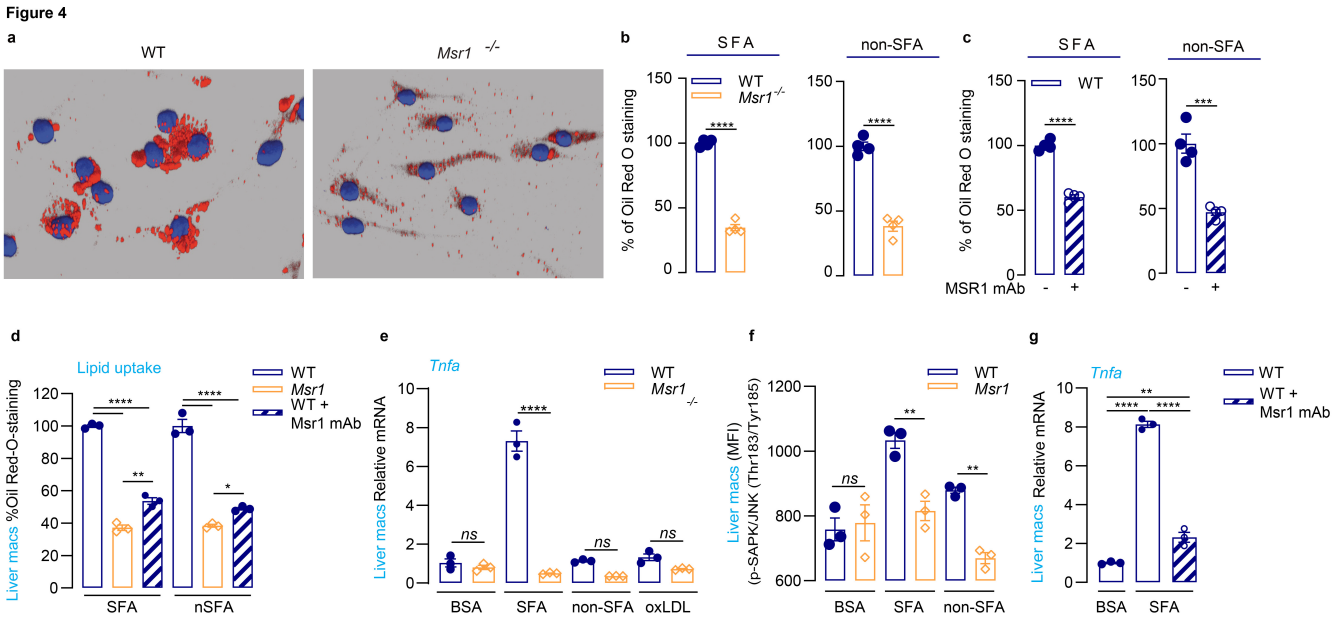

Fig. 4. Msr1 regulates JNK-mediated lipid-induced pro-inflammatory activation of macrophages. (**a**) Representative image of lipid uptake (mixture of 1mM Palmitic acid, saturated fatty acids (SFA), and 2mM Oleic, non-saturated fatty acids (non-SFA)) by WT and *Msr1*$^{-/-}$ bone marrow derived macrophages (BMDMs) visualized by Oil-red-O staining using confocal microscopy (n=3). (**b-c**) Quantification of SFA (palmitic acid 1mM) and non-SFA (oleic acid 2mM) uptake either by WT and *Msr1*$^{-/-}$ BMDMs, or WT BMDMs pre-treated with or without monoclonal anti-Msr1 antibody using Oil-red-O staining (n=4). Data are normalized to the average of the WT BMDM group. (**d**) Quantification of Oil-red-O staining to assess the uptake of SFA (palmitic acid 1mM) and non-SFA (oleic acid 2mM) by WT and *Msr1*$^{-/-}$ primary liver macrophages, or WT primary liver macrophages pre-treated with or without monoclonal anti-Msr1 antibody (n=4). Data are normalized to the average of the WT BMDM group. (**e**) Real time-PCR analysis of *Tnfa* pro-inflammatory gene in WT and *Msr1*$^{-/-}$ primary liver macrophages treated either with control bovine serum albumin (BSA) or SFA, non-SFA or oxidized low-density lipoprotein (oxLDL) for 6hrs (n=3). (**f**) Flow cytometry analysis of phospho-JNK (Thr183/Tyr185) in WT and *Msr1*$^{-/-}$ primary liver macrophages treated either with BSA as control or SFA and non-SFA for 3hrs (n=3). (**g**) Real time-PCR analysis of *Tnfa* expression in WT primary liver macrophages pre-treated with or without monoclonal anti-Msr1 antibody (n=3). Data are shown as mean ± SEM (unpaired Student's t-test or one-way ANOVA with correction for multiple testing; for panel d-f, the p-values are shown only for grouped comparisons per experimental condition; *p< 0.05, **p < 0.01, ***p < 0.001, ****p < 0.0001).

Figure 5

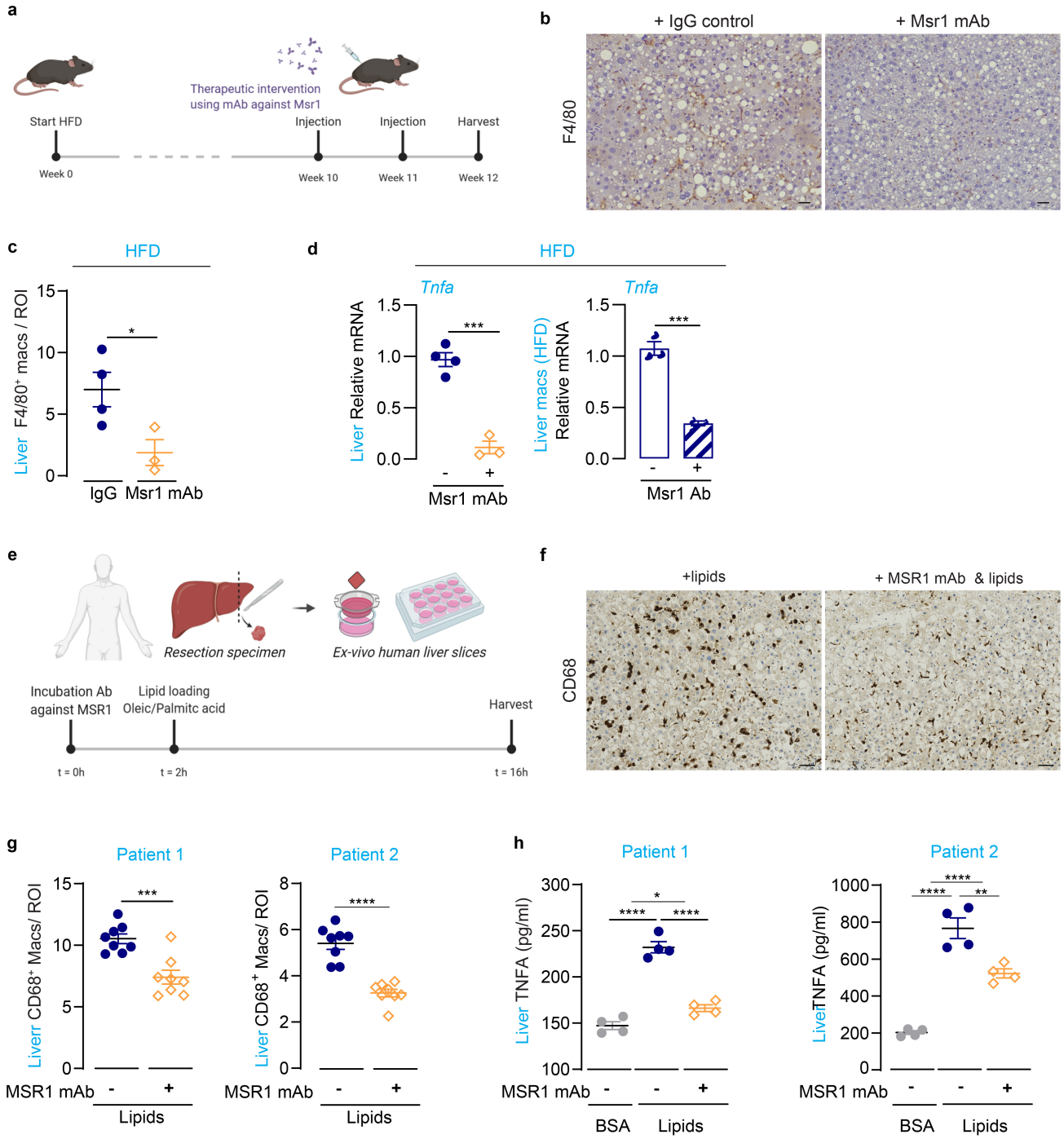

Figure 5. Therapeutic inhibition of MSR1 prevents formation of pro-inflammatory foamy macrophages. (**a**) Schematic overview of therapeutic antibody-based intervention in a NAFLD mouse model. (**b**) Immunohistochemical staining of liver samples for F4/80 from HFD-fed animals treated with anti-Msr1 antibody (n=3) or IgG control (n=4). (**c**) Quantification of F4/80 staining from treated animals presented as percentage pixel positivity of the region of interest (ROI). (**d**) Real-time PCR analysis for *Tnfa* transcript in liver samples and isolated

881 hepatic macrophages from HFD-fed animals treated with anti-Msr1 antibody (n=3) or IgG control (n=4). Isolated
882 primary liver macrophages were pooled together before real-time PCR analysis (n=3). (**e**) Schematic overview of
883 antibody-based treatment of *ex vivo* lipid-loaded human liver slices. Per patient, two biological replicates were used
884 for each condition. Samples were loaded with a combination of oleic (2mM) and palmitic acid (1mM). (**f**)
885 Immunohistochemical staining for CD68 on human lipid-loaded liver slices treated with or without anti-MSR1
886 antibody. (**g**) Quantification of CD68 staining (4 areas per liver slice) presented as percentage pixel positivity of the
887 region of interest (ROI). (h) TNFα ELISA from human liver slices treated with control Bovine Serum Albumin
888 (BSA), lipids or anti-MSR1-antibody+lipids (two technical measurements were performed per biological replicate).
889 Data are presented as mean ± SEM (unpaired Student's t-test or one-way ANOVA with correction for multiple
890 testing; *$p < 0.05$, **$p < 0.01$, ***$p < 0.001$, ****$p < 0.0001$). Scale bars 50µm.
891

Figure 6

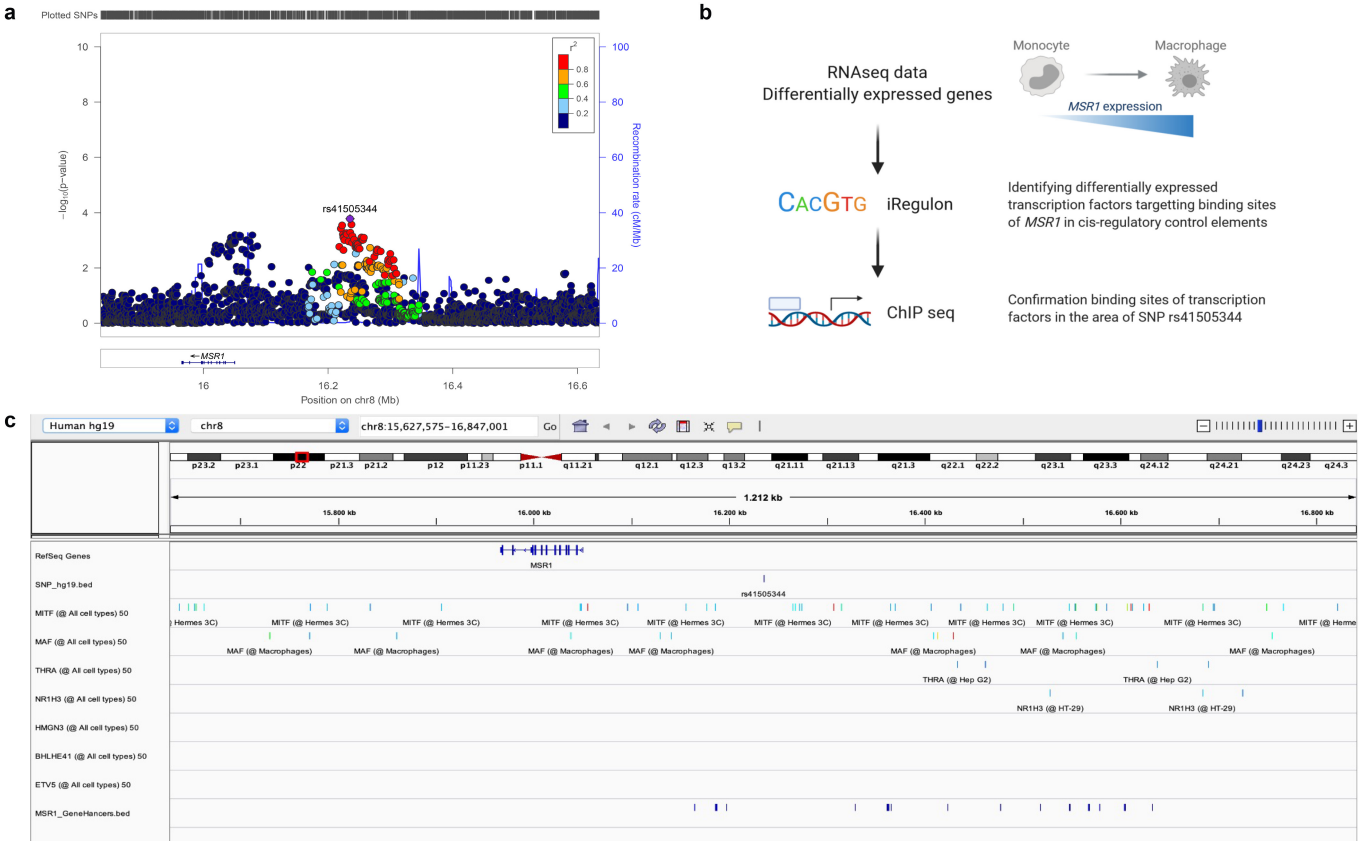

Figure 6. Regulatory mechanisms of *MSR1* expression in human NAFLD.

(**a**) Locus plot showing *MSR1* rs41505344 SNP based on case-control analysis comparing 1,483 histologically characterized NAFLD samples with 17,781 matched population controls. (**b**) Schematic overview of the workflow used to identify transcriptional regulatory mechanisms of *MSR1* from publicly available RNA sequencing data, comparing human monocytes with differentiated macrophages (*24*). (**c**) Visualization of chromatin immunoprecipitation sequencing data around *MSR1* rs41505344 SNP of the predicted transcription factors that are differentially expressed in the RNA sequencing data as identified by iRegulon. Bottom row indicates known transcriptional regulatory regions of *MSR1*.

902 **Table 1.** Correlation rs41505344 SNP with clinical features using UK Biobank (n=430,101)
903

			rs41505344_*MSR1*						Unadjusted	Adjusted for age, gender, BMI, PC 1-10, Assessment center and array batch		
			GG		GA		AA			Inverse normal rank transformation		
Characteristic	**Value**	**Range**	**Value**	**Range**	**Value**	**Range**	**Value**	**Range**	**p-value**	**p-value**	**Beta**	**CI**
n-value	430101		344142		81079		4880					
Age, y (mean ± SD)	56.8±8.03	39-73	56.8±8.03	39-72	56.8±8.02	39-73	56.7±8.06	40-70	0.80			
BMI, kg/m2 (mean ± SD)	27.4±4.76	12.1-74.7	27.4±4.77	12.6-68.4	27.4±4.75	12.1-74.7	27.3±4.81	16.2-54.5	0.02			
Male, n (%)	196727 (45.7)		157394 (45.7)		37080 (45.7)		2253 (46.2)		0.80			
ALT (U/L)	23.5±14.1	3.01-495	23.6±14.1	3.1-495	23.5±14.3	3.01-472	23.3±13.1	3.82-286	0.01	0.063	-0.0060	
AST (U/L)	26.2±10.6	3.3-947	26.2±10.5	3.3-947	26.2±11	3.3-711	26±9.72	8.4-227	8.29E-04	0.003	-0.010	
Glucose (mM)	5.12±1.21	1-36.8	5.12±1.2	1.1-36.8	5.12±1.23	1-32.7	5.12±1.18	1.8-22.3	0.76	0.41	0.003	
Cholesterol (mM)	5.71±1.14	0.601-15.5	5.71±1.14	0.601-15.5	5.71±1.14	1.71-13.3	5.68±1.13	2.39-12.3	0.16	0.12	-0.005	
LDL (mM)	3.57±0.87	0.266-9.8	3.57±0.87	0.266-9.8	3.57±0.868	0.751-9.61	3.55±0.862	1.22-7.64	0.16	0.15	-0.0051	
HDL cholesterol (mM)	1.45±0.382	0.219-4.4	1.45±0.382	0.226-4.4	1.46±0.382	0.219-4.13	1.45±0.38	0.628-3.22	0.03	0.071	0.006	
Triglycerides (mM)	1.75±1.02	0.231-11.3	1.76±1.03	0.233-11.3	1.74±1.02	0.231-11.3	1.72±1	0.375-11	8.27E-07	3.55E-06	-0.015	
Chronic liver disease, n (%)	6024 (1.401)		4807 (1.397)		1161 (1.432)		56 (1.148)		0.98	0.92	1.003	0.946-1.06
All-cause cirrhosis, n (%)	1709 (0.397)		1349 (0.392)		344 (0.424)		16 (0.328)		0.40	0.37	1.051	0.943-1.17

904